

Addressing Strong Correlation by Approximate Coupled-Pair Methods with Active-Space and Full Treatments of Three-Body Clusters

Ilias Magoulas,¹ Jun Shen,¹ and Piotr Piecuch^{1,2,*}

¹*Department of Chemistry, Michigan State University,
East Lansing, Michigan 48824, USA*

²*Department of Physics and Astronomy,
Michigan State University, East Lansing, Michigan 48824, USA*

(Dated: November 30, 2021)

Abstract

When the number of strongly correlated electrons becomes larger, the single-reference coupled-cluster (CC) CCSD, CCSDT, *etc.* hierarchy displays an erratic behavior, while traditional multi-reference approaches may no longer be applicable due to enormous dimensionalities of the underlying model spaces. These difficulties can be alleviated by the approximate coupled-pair (ACP) theories, in which selected $(T_2)^2$ diagrams in the CCSD amplitude equations are removed, but there is no generally accepted and robust way of incorporating connected triply excited (T_3) clusters within the ACP framework. It is also not clear if the specific combinations of $(T_2)^2$ diagrams that work well for strongly correlated minimum-basis-set model systems are optimum when larger basis sets are employed. This study explores these topics by considering a few novel ACP schemes with the active-space and full treatments of T_3 correlations and schemes that scale selected $(T_2)^2$ diagrams by factors depending on the numbers of occupied and unoccupied orbitals. The performance of the proposed ACP approaches is illustrated by examining the symmetric dissociations of the H_6 and H_{10} rings using basis sets of the triple- and double- ζ quality and the H_{50} linear chain treated with a minimum basis, for which the conventional CCSD and CCSDT methods fail.

* Corresponding author; e-mail: piecuch@chemistry.msu.edu.

I. INTRODUCTION

The size extensive methods based on the exponential wave function ansatz [1, 2] of coupled-cluster (CC) theory [3–8],

$$|\Psi\rangle = \exp(T)|\Phi\rangle, \quad (1)$$

where

$$T = \sum_{n=1}^N T_n \quad (2)$$

is the cluster operator, T_n is the n -particle– n -hole component of T , N is the number of correlated electrons, and $|\Phi\rangle$ is the reference (*e.g.*, Hartree–Fock) determinant defining the Fermi vacuum, have become a *de facto* standard for high-accuracy quantum chemistry calculations [9, 10]. This is, in significant part, related to the fact that the conventional single-reference CC hierarchy, including the CC approach with singles and doubles (CCSD), where T is truncated at T_2 [11–14], the CC method with singles, doubles, and triples (CCSDT), where T is truncated at T_3 [15–17], the CC approach with singles, doubles, triples, and quadruples (CCSDTQ), where T is truncated at T_4 [18–21], *etc.*, and its extensions to excited states and properties other than energy through the equation-of-motion [22–29] and linear response [30–38] formalisms rapidly converge to the exact, full configuration interaction (FCI), limit in weakly correlated systems. Higher-order CC methods, such as CCSDT and CCSDTQ, can also describe multi-reference situations involving smaller numbers of strongly correlated electrons, encountered, for example, when single and double bond dissociations are examined, allowing one to capture the relevant many-electron correlation effects in a conceptually straightforward fashion through particle–hole (p–h) excitations from a single determinant.

Unfortunately, the conventional CCSD, CCSDT, CCSDTQ, *etc.* hierarchy may exhibit an erratic behavior and the lack of systematic convergence toward the exact, FCI, limit, if the system under consideration is characterized by the strong entanglement of larger numbers of electrons, as in the Mott metal–insulator transitions [39–41], which can be modeled by the Hubbard Hamiltonian [42–44] (see, *e.g.*, Refs. [45, 46] and references therein) or the linear chains, rings, or cubic lattices of the equally spaced hydrogen atoms that change from a weakly correlated metallic state at compressed geometries to an insulating state with strong correlations in the dissociation region (see, *e.g.*, Refs. [47–54]). The analogous challenges apply to the strongly correlated π -electron networks in cyclic polyenes [55, 56],

as described by the Hubbard and Pariser–Parr–Pople (PPP) [57–59] Hamiltonians, which can be used to model one-dimensional metallic-like systems with Born–von Kármán periodic boundary conditions and a half-filled band [60–67]. When the numbers of strongly correlated electrons and open-shell sites from which these electrons originate become larger, traditional multi-reference methods of the CC [9, 10, 68–71] and non-CC [72–74] types, which typically build upon complete active-space self-consistent field (CASSCF) [75, 76], become inapplicable as well (in part, due to rapidly growing dimensionalities of the underlying multi-configurational reference or model spaces with the numbers of active electrons and orbitals, which are further complicated by considerable additional computational costs of determining the remaining dynamical correlation effects needed to obtain a quantitative description). Even the increasingly popular and undoubtedly promising substitutes for CASSCF, such as the density-matrix renormalization group (DMRG) approach [77–83] (*cf.* Ref. [84] for a recent perspective), FCI Quantum Monte Carlo [85–89], and various selected CI techniques [90–104], or methods that replace complete active spaces by their incomplete or multi-layer counterparts (*cf.*, *e.g.*, Refs. [105–110] for selected examples), which allow one to use significantly larger numbers of active electrons and orbitals compared to CASSCF-based schemes, begin to wear out when the number of strongly correlated electrons is on the order of 40–50. This is especially true when one wants to capture the missing dynamical correlations (*cf.*, *e.g.*, Refs. [111–116]) and use basis sets much larger than the minimum one. While there has been a lot of activity directed toward addressing these and related issues, the challenge of strong correlation remains, awaiting a satisfactory solution. It is, therefore, desirable to explore various unconventional methodologies capable of accurately describing weak as well as strong correlation regimes, especially those that formally belong to the single-reference CC framework, which is characterized by an ease of implementation and application that cannot be matched by genuine multi-reference theories. To do this, one has to understand the origin of the erratic behavior of conventional single-reference CC approaches in the presence of strong correlations.

The catastrophic failures of the traditional CCSD, CCSDT, CCSDTQ, *etc.* hierarchy in all of the aforementioned and similar situations, relevant to condensed matter physics, materials science, and the most severe cases of multiple bond breaking (*e.g.*, the celebrated chromium dimer), are related to the observation that in order to describe wave functions for N strongly correlated electrons one is essentially forced to deal with a FCI-level description

of these N electrons, which in a conventional CC formulation requires the incorporation of virtually all cluster components T_n , including T_N . Indeed, as shown, for example, in Fig. 2 of Ref. [117], using the 12-site, half-filled attractive pairing Hamiltonian with equally spaced levels, or slide 17 of Ref. [118], in which the 10-site Hubbard Hamiltonian with half-filled band is examined, the higher-order T_n components of the cluster operator, which normally decrease with n , remain large for larger n values approaching N in a strongly correlated regime. This is not a problem for the single-reference CC ansatz when the number of strongly correlated electrons N is small (*e.g.*, 2 in single bond breaking or 4 in double bond breaking), but becomes a major issue when N is larger.

The consequences of the above observations manifest themselves in various, sometimes dramatic, ways. For example, one experiences a disastrous behavior of the traditional CCSD, CCSDT, CCSDTQ, *etc.* hierarchy, which produces large errors, branch point singularities, and unphysical complex solutions in calculations for strongly correlated one-dimensional systems modeled by the Hubbard and PPP Hamiltonians or H_n rings, linear chains, and cubic lattices undergoing metal–insulator transitions [54, 60–67, 117, 119–121]. One can also show, using spin-symmetry breaking and restoration arguments, combined with the Thouless theorem [122, 123] and a subsequent cluster analysis [124] of projected unrestricted Hartree–Fock (PUHF) wave functions similar to Refs. [125, 126], that if we insist on the wave function ansatz in terms of the T_2 cluster component, the resulting strongly correlated PUHF state has a non-intuitive polynomial rather than the usual exponential form [127–129] (*cf.*, also, Refs. [117, 120, 121]). This means that in seeking a computationally manageable CC-type solution to a problem of strong correlation involving the entanglement of many electrons, which would avoid the combinatorial scaling of FCI while eliminating failures of the CCSD, CCSDT, CCSDTQ, *etc.* hierarchy, one has to resign from the conventional CC treatments in which the cluster operator T is truncated at a given many-body rank and all terms resulting from the exponential wave function ansatz are retained.

Among the most interesting solutions in this category are the approaches discussed in Refs. [117, 119–121, 127–139]. Another promising direction, which is the focus of this study, is the idea of the approximate coupled-pair (ACP) approaches [60–67, 125, 126, 140–146] and their various more recent reincarnations or modifications, including the 2CC approach and its n CC extensions [147, 148], the orbital invariant coupled electron pair approximation with an extensive renormalized triples correction [149], the parameterized CCSD methods [150]

and their CCSDT-type counterparts [151], and the distinguishable cluster approximation with doubles (DCD) or singles and doubles (DCSD) [52, 152–155] (see, also, Refs. [156–158]) and its DCSD(T) [154] and DCSDT [151, 159, 160] extensions to connected triples (see Ref. [161] for a review). At the doubles or singles and doubles levels, the ACP methods have the relatively inexpensive $n_o^2 n_u^4$ or \mathcal{N}^6 computational costs similar to CCD/CCSD, but by using the appropriately chosen subsets of non-linear $(T_2)^2$ diagrams of the CCD/CCSD amplitude equations, they greatly improve the performance of CCD/CCSD in strongly correlated situations, including single and multiple bond dissociations [52, 150, 152–156, 162] and, what is particularly intriguing, the low-dimensional metallic-like systems and symmetrically stretched hydrogen rings, linear chains, and cubic lattices, where the conventional CC treatments completely break down [52, 60–67] (we use the usual notation in which n_o and n_u are the numbers of correlated occupied and unoccupied orbitals, respectively, and \mathcal{N} is a measure of the system size). As further elaborated on in Section II, these improvements in the performance of conventional single-reference CC approaches are not a coincidence. One can prove that there exist subsets of CCSD diagrams that result in an exact description of certain strongly correlated minimum-basis-set model systems [64, 125, 126], *i.e.*, the ACP methodologies provide a rigorous basis for developing relatively inexpensive CC-like schemes for strong correlations (a multi-reference extension of the ACP ideas can also help genuine multi-reference CC approaches, especially when multi-determinantal model spaces become inadequate [163], but in this study we focus on the single-reference ACP framework).

Having stated all of the above, there remain several open problems that need to be addressed before the ACP methods can be routinely applied to realistic strongly correlated systems, *i.e.*, systems involving larger numbers of strongly correlated electrons described by *ab initio* Hamiltonians and larger basis sets. One of the main problems is the neglect of connected triply excited (T_3) clusters in typical ACP methods. The low-dimensional model systems with small band gaps, such as the aforementioned cyclic polyenes near their strongly correlated limits, do not suffer from this a lot [63, 65], since their accurate description relies on T_n clusters with even values of $n > 2$, but one cannot produce quantitative results in the majority of realistic chemistry applications without T_3 . The previous attempts to incorporate connected triply excited clusters within the ACP framework using conventional arguments based on the many-body perturbation theory (MBPT), similar to those exploited in $\text{CCD}[\text{ST}] \equiv \text{CCD} + \text{ST}(\text{CCD})$ [164], $\text{CCSD}[\text{T}] \equiv \text{CCSD} + \text{T}(\text{CCSD})$ [165], $\text{CCSD}(\text{T})$ [166],

or CCSDT-1 [167, 168], have only been partly successful [63, 65, 66, 126, 146, 154]. They improved the ACP results in the weakly and moderately correlated regions of the cyclic polyene models, but did not help in the strongly correlated regime [63, 65]. The aforementioned proposals how to include connected triply excited clusters in the parameterized CCSD and DCSD methods [151, 154, 159, 160] and the n CC approaches with $n > 2$, which incorporate T_3 as well [147, 148], while being helpful in some cases of bond breaking, have never been applied to strongly correlated systems involving the entanglement of larger numbers of electrons. Thus, it remains unclear how to produce a computationally efficient ACP-type procedure that would include the information about connected triply excited clusters and work well in such situations at the same time. Another open problem pertains to the fact that the specific combinations of $(T_2)^2$ diagrams that result in the ACP methods that work well in the strongly correlated regime of the minimum-basis-set model systems, such as the π -electron networks of cyclic polyenes, as described by the Hubbard and PPP Hamiltonians [60–67, 125, 126, 140] (see Section II for further information), may not necessarily be optimum when larger basis sets are employed.

We examine both of these topics in the present study. We deal with the problem of the missing T_3 physics by adopting the active-space CC ideas [21, 25, 26, 169–189] to incorporate the dominant triply excited amplitudes in the ACP methods in a robust, yet computationally affordable, manner. We show that the active-space triples ACP approaches examined in this work, which, following the naming convention introduced in Refs. [177, 178], are collectively abbreviated as ACCSDt, do not suffer from the previously observed [63, 65] convergence problems resulting from the use of MBPT-based estimates of T_3 contributions within the ACP framework in a strongly correlated regime. Furthermore, by incorporating the leading triply excited cluster amplitudes in an iterative manner, the ACCSDt methods developed in this study allow the T_1 and T_2 clusters and, in particular, the subsets of $(T_2)^2$ contributions responsible for an accurate description of strong correlations, to relax in the presence of the dominant T_3 amplitudes. The active-space ACCSDt schemes are also characterized by the systematic convergence toward their ACCSDT parents, in which T_3 clusters are treated fully, when the numbers of active occupied and active unoccupied orbitals used in the ACCSDt calculations increase. The issue of adjusting the $(T_2)^2$ diagram combinations in the ACP amplitude equations to the numbers of occupied and unoccupied orbitals used in the calculations is explored in this study by testing a novel form of the ACP theory, abbre-

viated as $\text{ACCSd}(1, 3 \times \frac{n_o}{n_o+n_u} + 4 \times \frac{n_u}{n_o+n_u})$, and its extensions accounting for T_3 correlations, abbreviated as $\text{ACCSdt}(1, 3 \times \frac{n_o}{n_o+n_u} + 4 \times \frac{n_u}{n_o+n_u})$ and $\text{ACCSdT}(1, 3 \times \frac{n_o}{n_o+n_u} + 4 \times \frac{n_u}{n_o+n_u})$, which utilize the n_o - and n_u -dependent scaling factors multiplying the $(T_2)^2$ diagrams kept in the calculations. At the singles and doubles level and when $n_o = n_u$, *i.e.*, when a minimum basis set is employed, the $\text{ACCSd}(1, 3 \times \frac{n_o}{n_o+n_u} + 4 \times \frac{n_u}{n_o+n_u})$ scheme reduces to the DCSD approach of Ref. [52], which, in analogy to the closely related ACP-D13 and ACP-D14 methods introduced in Ref. [64], becomes exact in the strongly correlated limit of cyclic polyenes modeled by the Hubbard and PPP Hamiltonians. At the same time, the $\text{ACCSdT}(1, 3 \times \frac{n_o}{n_o+n_u} + 4 \times \frac{n_u}{n_o+n_u})$ approach becomes equivalent to the ACP-D14 method of Ref. [64] augmented with T_1 and T_3 clusters when $n_o \ll n_u$, which does, based on our numerical tests, including those discussed in Section III, improve the $\text{ACCSdT}(1, \frac{3+4}{2})$ results, obtained by embedding $\text{ACCSd}(1, \frac{3+4}{2}) = \text{DCSD}$ in CCSDT, in calculations using larger basis sets. By examining the symmetric dissociations of the H_6 and H_{10} rings, as described by basis sets of the triple- and double- ζ quality, for which the exact, FCI, calculations are feasible, and the H_{50} linear chain treated with a minimum basis, for which the nearly exact, DMRG, results are available [47], we show that the active-space $\text{ACCSdt}(1, 3 \times \frac{n_o}{n_o+n_u} + 4 \times \frac{n_u}{n_o+n_u})$ method and its $\text{ACCSdT}(1, 3 \times \frac{n_o}{n_o+n_u} + 4 \times \frac{n_u}{n_o+n_u})$ parent accurately reproduce the FCI (H_6 and H_{10}) and DMRG (H_{50}) energetics, while improving the $\text{ACCSd}(1, 3 \times \frac{n_o}{n_o+n_u} + 4 \times \frac{n_u}{n_o+n_u})$ results and eliminating catastrophic failures of CCSD and CCSDT in the strongly correlated regions. Because of the use of basis sets larger than a minimum one in calculations for the H_6 and H_{10} ring systems, we also demonstrate that $\text{ACCSdt}(1, 3 \times \frac{n_o}{n_o+n_u} + 4 \times \frac{n_u}{n_o+n_u})$ and other ACCSdt schemes recover the corresponding ACCSDT results, including a strongly correlated regime, at the tiny fraction of the computational cost.

II. THEORY AND COMPUTATIONAL DETAILS

A. Overview of the ACP Schemes

Historically, a variety of different ways of rationalizing the ACP and related methods using subsets of non-linear diagrams within a CCD/CCSD framework have been considered (*cf.* Refs. [52, 60, 64, 65, 125, 126, 140–145, 147–150, 161]). Given the objectives of this study, we begin our discussion with the past numerical observations and mathematical analyses that

allow us to understand the ability of such methods to describe strongly correlated electrons. Let us focus for a moment on a simpler CCD case, so that we do not have to worry about the less essential, but more numerous, contributions containing the T_1 cluster component. Using the language of Goldstone–Brandow (Goldstone–Hugenholtz) diagrams, utilized in the derivations whenever the orthogonally spin-adapted description [14, 34, 125, 126, 140, 190–197], important for the understanding of the earliest ACP models, is desired, one may show that of the five Goldstone–Brandow $(T_2)^2$ diagrams of the CCD amplitude equations,

$$s_r \langle \Phi_{IJ}^{AB} | [H_N(1 + T_2 + \frac{1}{2}T_2^2)]_C | \Phi \rangle = s_r \langle \Phi_{IJ}^{AB} | [H_N(1 + T_2)]_C | \Phi \rangle + \sum_{k=1}^5 \Lambda_k^{(2)}(AB, IJ; S_r) = 0, \quad (3)$$

represented in Eq. (3) by the $\Lambda_k^{(2)}(AB, IJ; S_r)$, $k = 1-5$, terms and shown in Fig. 1 as diagrams (1)–(5), only two, namely, diagrams (4) and (5), which are separable over the hole line(s), are needed to eliminate the pole singularities plaguing linearized CCD in situations involving electronic quasi-degeneracies [60–62, 141–143]. Here, we use the notation in which $H_N = H - \langle \Phi | H | \Phi \rangle$ is the Hamiltonian in the normal-ordered form and subscript C indicates the connected operator product. The $|\Phi_{IJ}^{AB}\rangle_{S_r}$ states in Eq. (3), where I and J designate the occupied and A and B the unoccupied spatial orbitals in the closed-shell reference determinant $|\Phi\rangle$ and $S_r = 0$ or 1 is the intermediate spin quantum number, represent the singlet particle-particle–hole-hole (pp–hh) coupled orthogonally spin-adapted doubly excited configuration state functions (CSFs). Using these functions, the T_2 operator entering Eq. (3), represented in Fig. 1 by the oval-shaped vertices, is defined as

$$T_2|\Phi\rangle = \sum_{I \leq J, A \leq B} \sum_{S_r=0}^1 t_{AB}^{IJ}(S_r) |\Phi_{IJ}^{AB}\rangle_{S_r} = \frac{1}{4} \sum_{IJAB} \sum_{S_r=0}^1 (N_{IJ}^{AB})^{-2} t_{AB}^{IJ}(S_r) |\Phi_{IJ}^{AB}\rangle_{S_r}, \quad (4)$$

where $t_{AB}^{IJ}(S_r)$ are the corresponding spin-adapted doubly excited cluster amplitudes and

$$N_{IJ}^{AB} = [(1 + \delta_{IJ})(1 + \delta_{AB})]^{-1/2}, \quad (5)$$

with δ_{IJ} and δ_{AB} designating Kronecker deltas, is the appropriate normalization factor [14, 125, 126, 140, 191–193]. The ACP approach obtained using only the 4th and 5th $(T_2)^2$ contributions in Eq. (3), $\Lambda_4^{(2)}(AB, IJ; S_r)$ and $\Lambda_5^{(2)}(AB, IJ; S_r)$, respectively, has originally been called ACP-D45 [141–143] or ACCD [144, 145]. As shown in Refs. [60–62, 141–145], using the aforementioned cyclic polyene models, C_NH_N , in a π -electron approximation, described by the Hubbard and PPP Hamiltonians, where one places $N = 4n + 2$, $n = 1, 2, \dots$,

carbon atoms on a ring, and several *ab initio* systems, including small hydrogen clusters, beryllium atom, and small molecules, the ACP-D45 method is as accurate as CCD in weakly correlated cases with no electronic quasi-degeneracies, while representing an excellent approximation in strongly correlated, highly degenerate situations, where the linearized CCD [60–62, 141–143] or even the full CCD [60–66], CCD corrected for connected triples via perturbative approximations of the CCD[ST] or CCSD[T] and CCSDT-1 types [63, 65, 66], CCSDT [67], and CCSDTQ [67] are plagued with singularities or divergent behavior. At the time of the initial discovery of the ACP-D45 or ACCD scheme, this remarkable behavior was partially explained by the mutual cancellation of the contributions arising from the first three diagrams in Fig. 1, observed numerically [60, 141–143] and advocated mathematically by considering the limit of non-interacting electron pairs [144]. However, this could not explain why the ACP-D45 approach, using only two of the five $(T_2)^2$ Goldstone–Brandow diagrams of CCD, works so well in the strongly correlated, $\beta = 0$, limit of the cyclic polyene models, where CCD completely fails, producing branch point singularities and complex solutions for cyclic polyenes with 14 or more carbon sites as β approaches 0 from the weakly correlated $\beta \ll 0$ region [60–66] (β is the parameter scaling the one-electron part of the Hubbard or PPP Hamiltonians; in the Hubbard Hamiltonian case, β is equivalent to $-t/U$, where t and U are the parameters controlling the kinetic energy characterizing the hopping of electrons between nearest neighbors and on-site electron-electron repulsion, respectively). In fact, it was observed that ACP-D45 is exact in the strongly correlated, $\beta = 0$, limit of the Hubbard model [60–66], while being accurate for the PPP Hamiltonian and other β values. Other selections of CCD or CCSD $(T_2)^2$ diagrams were considered by several authors in recent years [52, 147, 148, 150, 152–158], with some choices being similar or even identical to the original ACP approaches examined in Refs. [60–67, 125, 126, 140–146], seeking diagram combinations that work better than CCD/CCSD in bond breaking situations, but none of these recent studies have provided rigorous mathematical arguments why the ACP methods, such as ACP-D45, can be exact or nearly exact in strongly correlated situations of the type of those created by the cyclic polyene models in the $\beta \approx 0$ region.

The major breakthrough in the understanding of the superb performance of the ACP-D45 approach in a strongly correlated regime came in 1984 [125], followed by two other key articles published in 1991 [64] and 1996 [126]. By performing cluster analysis [124] of the PUHF wave function within the orthogonally spin-adapted framework, in which the PUHF

state was assumed to be exact, and using the philosophy of the externally corrected CC methods [125, 126, 161, 198–209], the authors of Refs. [125, 126] demonstrated that the T_4 cluster component extracted from PUHF with the help of the Thouless theorem and read into the CCD system, Eq. (3), (Ref. [125]) or its CCSD extension (Ref. [126]) as the $s_r \langle \Phi_{IJ}^{AB} | (H_N T_4)_C | \Phi \rangle$ contribution cancels out the first three of the five diagrams in Fig. 1, while multiplying the fifth diagram in the equations projected on the singlet pp–hh coupled orthogonally spin-adapted doubly excited $|\Phi_{IJ}^{AB}\rangle_{S_r}$ CSFs with the intermediate spin $S_r = 1$ by a factor of 9 (in principle, the analogous T_3 -containing contributions should have been read into the CCD or CCSD systems too, but they were not, since T_3 extracted from the PUHF wave function, represented as a CC state relative to the restricted Hartree–Fock (RHF) reference determinant, vanishes [125, 126]). The PUHF wave function provides exact energies and cluster amplitudes for the PPP and Hubbard Hamiltonian models of cyclic polyenes in the strongly correlated, $\beta = 0$, limit, so the resulting ACP-D45₉ theory, abbreviated as ACPQ [125] or ACCD' [126], using $\Lambda_4^{(2)}(AB, IJ; S_r) + (2S_r + 1)^2 \Lambda_5^{(2)}(AB, IJ; S_r)$ instead of $\sum_{k=1}^5 \Lambda_k^{(2)}(AB, IJ; S_r)$ to represent the $(T_2)^2$ contributions within the CCD system, Eq. (3), is mathematically exact in this limit, in complete agreement with the numerical observations [60–67] (the T_1 contributions can be ignored here, since $T_1 = 0$ for the cyclic polyene models described by the PPP and Hubbard Hamiltonians). The aforementioned factor of 9, which is simply the square of the multiplicity associated with the intermediate spin value $S_r = 1$, was a result of using the orthogonally spin-adapted formalism; without using this formalism and without the exploitation of the appropriate many-body and angular momentum diagrammatic techniques in Refs. [125, 126], one would not be able to see the emergence of $(2S_r + 1)^2$ at the $\Lambda_5^{(2)}(AB, IJ; S_r)$ term corresponding to diagram (5) in a transparent manner. The original derivation in Ref. [125] assumed that the PUHF wave function has no singlet-coupled singly excited CSFs relative to RHF, which is true for the PPP and Hubbard Hamiltonian models of cyclic polyenes due to symmetry, but not in general, so the ACP-D45₉ = ACPQ = ACCD' scheme and its more complete CCSD-level extension, where the T_1 clusters are included as well, termed ACCSD' [126], were rederived in Ref. [126]. Reference [126] also examined the CCSDQ' approach and its triples-corrected CCSDQ' + T(CCSDQ') = CCSDQ'[T] extension, where one does not make any assumptions regarding the accuracy of PUHF and extracts the T_4 cluster component from a PUHF wave function as is, showing additional improvements in some cases, but our focus here is on the

philosophy represented by the ACP methods, such as ACCSD'. If the above factor of 9 at the fifth diagram in Fig. 1 for the $S_r = 1$ case is ignored (and for the cyclic polyene models, as described by the PPP and Hubbard Hamiltonians, $\Lambda_5^{(2)}(AB, IJ; S_r)$ is generally small), the ACP-D45₉ = ACPQ = ACCD' scheme, derived in Ref. [125] and extended to a singles and doubles level in Ref. [126], reduces to the original ACP-D45 or ACCD approach of Refs. [141–145]. In fact, in the strongly correlated, $\beta = 0$, limit of cyclic polyenes described by the Hubbard Hamiltonian, the $\Lambda_5^{(2)}(AB, IJ; S_r = 1)$ term vanishes [64], so that the ACP-D45 approximation becomes exact in this case, as observed numerically [60–66]. When the above factor of 9 is included, as in the ACP-D45₉ = ACPQ = ACCD' or ACCSD' approaches, one ends up with an exact description of the strongly correlated, $\beta = 0$, limit of cyclic polyenes with $4n + 2$ carbons on a ring and described by either the Hubbard or PPP Hamiltonians. This result is independent of n , *i.e.*, it remains valid in the thermodynamic limit.

There are other selections of the $(T_2)^2$ diagrams entering the CCD or CCSD amplitude equations that can also be exact in the strongly correlated regimes of model Hamiltonians. In Ref. [64], the exactness of ACP-D45₉ = ACPQ = ACCD' in the strongly correlated, $\beta = 0$, limit of the cyclic polyene models described by the Hubbard and PPP Hamiltonians was re-examined using back substitution of the exact T_2 amplitudes extracted from a PUHF wave function into the CCD and ACP-D45₉ systems. By doing so, it was proven that the exact T_2 amplitudes satisfy the latter system, but not the former one, showing that ACP-D45₉ is exact when $\beta = 0$ and CCD is not (as already mentioned, CCD behaves erratically in the $\beta = 0$ limit). Encouraged by the usefulness of such an analysis, the authors of Ref. [64] searched for other combinations of the CCD $(T_2)^2$ diagrams that produce exact results at $\beta = 0$, discovering several possibilities. One of them, using diagrams (1) and (4) in Fig. 1 and defining the ACP-D14 approach, is $\Lambda_1^{(2)}(AB, IJ; S_r) + \Lambda_4^{(2)}(AB, IJ; S_r)$. As shown in Ref. [64] for the cyclic polyene models, which have several symmetries, including the p–h symmetry, $\Lambda_3^{(2)}(AB, IJ; S_r) = \Lambda_4^{(2)}(AB, IJ; S_r)$, *i.e.*, diagrams (3) and (4) in Fig. 1 are equivalent in this case. Thus, one can also propose two other methods, ACP-D13 and ACP-D1(3+4)/2, which correspond to the following expressions for the $(T_2)^2$ contributions within a CCD or CCSD framework: $\Lambda_1^{(2)}(AB, IJ; S_r) + \Lambda_3^{(2)}(AB, IJ; S_r)$ and $\Lambda_1^{(2)}(AB, IJ; S_r) + [\Lambda_3^{(2)}(AB, IJ; S_r) + \Lambda_4^{(2)}(AB, IJ; S_r)]/2$, respectively. All three methods, ACP-D13, ACP-D14, and ACP-D1(3+4)/2, are exact in the strongly correlated, $\beta = 0$, limit of cyclic polyenes described by the Hubbard and PPP Hamiltonians, *i.e.*, it is worth considering

them all. The performance of the ACP-D14 approach in the calculations for cyclic polyenes in the entire range of β values, from the weakly to the strongly correlated regimes and systems as large as $\text{C}_{22}\text{H}_{22}$, was examined in Ref. [64], showing the excellent and non-singular behavior similar to the $\text{ACP-D45}_9 = \text{ACPQ} = \text{ACCD}'$ methods tested in Refs. [60–66]. The calculations using the other two approaches, ACP-D13 and $\text{ACP-D1(3+4)}/2$, were not reported in Ref. [64], since they would produce identical results due to the p–h symmetry intrinsic to the cyclic polyene models. The $\text{ACP-D1(3+4)}/2$ approach, rationalized by the 1991 analysis in Ref. [64], is equivalent to the recently pursued DCD method of Refs. [52, 152–155]. By averaging diagrams (3) and (4), which are the p–h versions of each other, the $\text{ACP-D1(3+4)}/2 = \text{DCD}$ model attempts to reinforce the p–h symmetry, even if there is none in the Hamiltonian. Time will tell if it is beneficial to do this in *ab initio* applications involving strongly correlated situations, that is, if using DCD and its CCSD-like extension, termed DCSD [52, 152–155], is an overall better idea than using the older $\text{ACP-D45}_9 = \text{ACPQ} = \text{ACCD}'$ and ACCS' approaches. The performance of the latter approach in bond breaking situations was examined as early as in 1996 [162], but our knowledge of the relative performance of these different ACP variants, especially in large-scale *ab initio* studies, is still rather limited, although various combinations of $(T_2)^2$ diagrams within CCSD have been examined in Refs. [52, 150, 152–156, 158], showing encouraging results.

There is no doubt that numerical tests of the various ACP-type approximations will continue to be helpful, but in order for these methods to become successful and widely used in the longer term, especially in the examination of problems involving larger numbers of strongly correlated electrons that cannot be handled by the existing multi-reference methods, selected CI, or DMRG, one has to address several issues. The above discussion implies that the ACP-D13 , ACP-D14 , $\text{ACP-D1(3+4)}/2 = \text{DCD}$, and $\text{ACP-D45}_9 = \text{ACPQ} = \text{ACCD}'$ approaches, obtained by considering subsets of $(T_2)^2$ diagrams within the CCD system, Eq. (3), and their extensions incorporating T_1 clusters are more robust than the traditional CCSD, CCSDT, CCSDTQ, *etc.* hierarchy in strongly correlated situations, but the main rationale behind their usefulness is based on considering strongly correlated limits of highly symmetric, minimum-basis-set, model Hamiltonians. It is not immediately obvious that the same combinations of $(T_2)^2$ diagrams remain optimum when larger basis sets, required by quantitative *ab initio* quantum chemistry, are employed. More importantly, as already explained above, the T_3 physics is absent in the ACP approaches derived within a CCD/CCSD framework or

its PUHF-driven externally corrected extensions, in which, as shown, for example, in Refs. [125, 126], $T_3 = 0$. In other words, the ACP methods obtained by selecting and modifying $(T_2)^2$ diagrams within CCD or CCSD, while capturing strong non-dynamical correlations in a computationally manageable fashion, even when the numbers of strongly correlated electrons are larger, and providing T_1 and T_2 clusters that are more accurate than those obtained with CCD or CCSD, offer incomplete information about dynamical correlation effects, which cannot be accurately described without the connected T_3 clusters. As pointed out in the Introduction, the previously developed ACP schemes corrected for the effects of connected triply excited clusters using arguments originating from MBPT [126, 140, 146] have only had partial success when examining cyclic polyene models [63, 65, 66], whereas the recent attempts to include T_3 correlations in parameterized CCSD and DCSD [151, 154, 159, 160] or via the n CC hierarchy [147, 148] have not been applied to strongly correlated systems involving the entanglement of larger numbers of electrons that interest us in this study most. It is, therefore, useful to consider alternative ways of handling connected triply excited clusters within the ACP methodology that might result in practical computational schemes, while having the potential for working well in a strongly correlated regime. We discuss such approaches in the next subsection.

B. The Proposed ACP Approaches

In searching for the combinations of $(T_2)^2$ diagrams that might potentially improve the ACP results corrected for T_3 correlations when larger basis sets are employed, it is worth noticing that one could retain the exactness of the ACP approaches using diagrams (1), (3), and (4) in Fig. 1 in the strongly correlated limit of cyclic polyenes, as described by the Hubbard and PPP Hamiltonians, by considering other combinations of diagrams (3) and (4) than those used in the ACP-D13, ACP-D14, and ACP-D1(3+4)/2 = DCD methods. One could, in fact, replace the $\sum_{k=1}^5 \Lambda_k^{(2)}(AB, IJ; S_r)$ contribution to the CCD system, Eq. (3), originating from the five $(T_2)^2$ diagrams shown in Fig. 1, by

$$\Lambda_1^{(2)}(AB, IJ; S_r) + \lambda \Lambda_3^{(2)}(AB, IJ; S_r) + (1 - \lambda) \Lambda_4^{(2)}(AB, IJ; S_r) \quad (6)$$

with an arbitrary value of λ , and still be exact in the $\beta = 0$ limit of the cyclic polyene models. In ACP-D1(3+4)/2 = DCD and its DCSD extension incorporating T_1 clusters,

one uses $\lambda = \frac{1}{2}$, which is appropriate for cyclic polyenes, as described by the Hubbard and PPP Hamiltonians that have the p-h symmetry, and justified in the case of other strongly correlated systems, such as the hydrogen clusters examined in this work described by the *ab initio* Hamiltonians, as long as one uses a minimum basis set, for which the p-h symmetry is approximately satisfied, but this does not necessarily mean that $\lambda = \frac{1}{2}$ is the optimum choice for larger basis sets, particularly when the predominantly dynamical T_3 correlations are included in the calculations. By numerically examining several strongly correlated systems treated with various basis sets, including the dissociating rings and linear chains composed of varying numbers of hydrogen atoms, such as those discussed in Section III, we have noticed that the ACP-D14 approximation, which uses $\lambda = 0$ in Eq. (6), works better when applied to the $(T_2)^2$ diagrams of the CCSDT amplitude equations projected on the doubly excited CSFs than its $\lambda = \frac{1}{2}$ ACP-D1(3+4)/2 = DCD counterpart when n_u is greater than n_o . This is especially true in the $n_u \gg n_o$ case, *i.e.*, when larger basis sets are employed. This observation suggests that in the case of the ACP approaches using diagrams (1), (3), and (4) of Fig. 1 within the CCSDT-type framework, it might be beneficial to scale up diagram (4) in Eq. (6) by decreasing the coefficient λ , *i.e.*, by increasing $(1 - \lambda)$ at $\Lambda_4^{(2)}(AB, IJ; S_r)$, when n_u becomes larger. The simplest expression for λ that allows us to accomplish this objective, while being invariant with respect to n_o and n_u if both of these numbers are simultaneously scaled by the same factor, is $\lambda = \frac{n_o}{n_o + n_u}$. At the singles and doubles level, the resulting ACP scheme, in which the $\sum_{k=1}^5 \Lambda_k^{(2)}(AB, IJ; S_r)$ contribution to the CCSD equations projected on the doubly excited CSFs is replaced by Eq. (6) with $\lambda = \frac{n_o}{n_o + n_u}$, is referred to as the ACCSD($1, 3 \times \frac{n_o}{n_o + n_u} + 4 \times \frac{n_u}{n_o + n_u}$) method. When $n_o = n_u$, the ACCSD($1, 3 \times \frac{n_o}{n_o + n_u} + 4 \times \frac{n_u}{n_o + n_u}$) scheme reduces to the DCSD approach, which is, in view of the above discussion, a desired behavior. At the same time, ACCSD($1, 3 \times \frac{n_o}{n_o + n_u} + 4 \times \frac{n_u}{n_o + n_u}$) becomes equivalent to the extension of the ACP-D14 approximation to the singles and doubles level when $n_u \rightarrow \infty$.

In analogy to the ACP-D13, ACP-D14, and ACP-D1(3+4)/2 approaches augmented with the T_1 clusters within a CCSD framework, abbreviated in this article as ACCSD(1,3), ACCSD(1,4), and ACCSD($1, \frac{3+4}{2}$), respectively, which correspond to setting λ in Eq. (6) at 1 [ACCSD(1,3)], 0 [ACCSD(1,4)], and $\frac{1}{2}$ [ACCSD($1, \frac{3+4}{2}$)], the ACCSD($1, 3 \times \frac{n_o}{n_o + n_u} + 4 \times \frac{n_u}{n_o + n_u}$) scheme is exact in the strongly correlated, $\beta = 0$, limit of cyclic polyenes, $C_{4n+2}H_{4n+2}$, as described by the Hubbard and PPP Hamiltonians, independent of the value

of n . Being equivalent to the DCSD method when $n_o = n_u$, it is also exact for two-electron systems or non-interacting electron pairs in a minimum basis set description. Although, unlike DCSD, the $\text{ACCS}(1, 3 \times \frac{n_o}{n_o+n_u} + 4 \times \frac{n_u}{n_o+n_u})$ approach is no longer exact for two-electron systems when $n_u > n_o$, the errors relative to FCI for species like H_2 and HeH^+ remain very small, on the order of 1–2 % of the correlation energy, even when $n_u \gg n_o$. Furthermore, as shown in Section III, using the symmetric dissociations of the H_6 and H_{10} rings as examples, the use of the $\text{ACCS}(1, 3 \times \frac{n_o}{n_o+n_u} + 4 \times \frac{n_u}{n_o+n_u})$ protocol within a CCSDT framework through the $\text{ACCS}(1, 3 \times \frac{n_o}{n_o+n_u} + 4 \times \frac{n_u}{n_o+n_u})$ approach and its active-space $\text{ACCS}(1, 3 \times \frac{n_o}{n_o+n_u} + 4 \times \frac{n_u}{n_o+n_u})$ counterpart, which we discuss next, in applications to strongly correlated systems described by basis sets larger than a minimum one improves the results compared to the ACCS and ACCS calculations that adopt the $(T_2)^2$ diagram selections defining $\text{ACCS}(1,3)$, $\text{ACCS}(1,4)$, and $\text{ACCS}(1, \frac{3+4}{2})$. While we will continue examining this theory aspect in the future, the benefits of applying the $\text{ACCS}(1, 3 \times \frac{n_o}{n_o+n_u} + 4 \times \frac{n_u}{n_o+n_u})$ approximation within a CCSDT-level description outweigh the loss of exactness in calculations for two-electron systems with $n_u > n_o$, especially when the errors relative to FCI are as small as mentioned above (and none when $n_u = n_o$).

Given the above discussion, we now move to the robust ways of incorporating T_3 correlations in the ACP schemes in which the $\sum_{k=1}^5 \Lambda_k^{(2)}(AB, IJ; S_r)$ contribution to the amplitude equations projected on the doubly excited CSFs is replaced by Eq. (6). Although our focus is on including the connected triply excited clusters in the $\text{ACCS}(1, 3 \times \frac{n_o}{n_o+n_u} + 4 \times \frac{n_u}{n_o+n_u})$ approach corresponding to $\lambda = \frac{n_o}{n_o+n_u}$ through the use of the active-space $\text{ACCS}(1, 3 \times \frac{n_o}{n_o+n_u} + 4 \times \frac{n_u}{n_o+n_u})$ approximation and its $\text{ACCS}(1, 3 \times \frac{n_o}{n_o+n_u} + 4 \times \frac{n_u}{n_o+n_u})$ parent, we discuss the analogous ACCS and ACCS extensions of the $\text{ACCS}(1,3)$, $\text{ACCS}(1,4)$, and $\text{ACCS}(1, \frac{3+4}{2}) = \text{DCSD}$ methods as well.

We recall that the main idea of all active-space CC methods and their excited-state and open-shell extensions is that of the selection of the leading higher-than-two-body components of the cluster and excitation operators, such T_3 or T_3 and T_4 , with the help of a small subset of orbitals around the Fermi level relevant to the quasi-degeneracy problem of interest [21, 25, 26, 169–185, 187–189] (see Ref. [186] for a review). Typically, this is accomplished by partitioning the spin-orbitals used in the calculations into the core, active occupied, active unoccupied, and virtual subsets and constraining the spin-orbital indices in the T_n cluster amplitudes with $n > 2$ and the corresponding excitation operators such that one can re-

produce the parent CCSDT, CCSDTQ, *etc.* energetics, including problems characterized by stronger multi-reference correlations, at the small fraction of the computational costs and with minimum loss of accuracy. In the leading approach in the active-space CC hierarchy, which was originally developed and implemented in Refs. [21, 170, 171, 173, 175] and which is nowadays abbreviated as CCSDt [177, 178], we approximate the cluster operator T by

$$T^{(\text{CCSDt})} = T_1 + T_2 + \mathbf{t}_3, \quad (7)$$

where T_1 and T_2 are the usual one- and two-body components of T , treated fully, and the three-body component \mathbf{t}_3 , written in the conventional spin-orbital notation in which i, j, k, \dots (a, b, c, \dots) designate the spin-orbitals occupied (unoccupied) in the reference determinant $|\Phi\rangle$, is defined as

$$\mathbf{t}_3|\Phi\rangle = \sum_{\substack{i < j < \underline{\mathbf{k}} \\ \underline{\mathbf{a}} < b < c}} t_{\underline{\mathbf{a}}bc}^{ijk} |\Phi_{ij\underline{\mathbf{k}}}^{\underline{\mathbf{a}}bc}\rangle. \quad (8)$$

The underlined bold indices in the triply excited cluster amplitudes $t_{\underline{\mathbf{a}}bc}^{ijk}$ and the corresponding triply excited determinants $|\Phi_{ij\underline{\mathbf{k}}}^{\underline{\mathbf{a}}bc}\rangle$ entering Eq. (8) denote active spin-orbitals in the respective categories ($\underline{\mathbf{k}}$ active occupied and $\underline{\mathbf{a}}$ active unoccupied ones). The singly, doubly, and triply excited amplitudes (or their spin-adapted counterparts) needed to determine the cluster operator $T^{(\text{CCSDt})}$, Eq. (7), are obtained in the usual way by projecting the electronic Schrödinger equation, with the CCSDt wave function $|\Psi^{(\text{CCSDt})}\rangle = \exp(T^{(\text{CCSDt})})|\Phi\rangle$ in it, on the excited Slater determinants (in the spin-adapted case, CSFs) corresponding to the content of $T^{(\text{CCSDt})}$. As in the case of all single-reference CC theories, the CCSDt energy is obtained by projecting the Schrödinger equation on the reference determinant $|\Phi\rangle$.

The CCSDt methodology has several features that are useful in the context of the ACP considerations pursued in this study. First, and foremost, it allows us to bring information about the leading T_3 correlations, which are absent in ACCSD(1,3), ACCSD(1,4), ACCSD(1, $\frac{3+4}{2}$) = DCSD, and ACCSD(1, $3 \times \frac{n_o}{n_o+n_u} + 4 \times \frac{n_u}{n_o+n_u}$), in a computationally efficient manner. Indeed, if N_o ($< n_o$) and N_u ($\ll n_u$) designate the numbers of the active occupied and active unoccupied orbitals, respectively, the CCSDt protocol, as briefly summarized above, replaces the expensive computational steps of the parent CCSDT treatment, which scale as $n_o^3 n_u^5$, by the much more manageable $N_o N_u n_o^2 n_u^4$ operations. At the same time, the CCSDt calculations reduce the $\sim n_o^3 n_u^3$ (*i.e.*, \mathcal{N}^6 -type) storage requirements associated with the full treatment of triply excited cluster amplitudes t_{abc}^{ijk} to the much less demanding

$\sim N_o N_u n_o^2 n_u^2$ (\mathcal{N}^4 -like) level. The $N_o N_u n_o^2 n_u^4$ computational steps of CCSDt, which are essentially equivalent to the polynomial, \mathcal{N}^6 -type, steps of CCSD multiplied by a relatively small prefactor proportional to the number of singles in the active space, are also much less expensive than typical costs of the CASSCF-based multi-reference CC or CI computations.

Another desirable feature of the CCSDt methodology is its non-perturbative character, which reduces the risk of introducing divergent behavior in a strongly correlated regime observed in the earlier ACP computations using MBPT-based treatments of triples [63, 65, 66]. The iterative character of CCSDt, which, unlike in the previously explored non-iterative triples corrections to the ACP and related DCSD approaches [63, 65, 66, 126, 140, 146, 154], allows one to adjust the T_1 and T_2 clusters, including the $(T_2)^2$ diagrams responsible for capturing strong correlations, to the dominant T_3 contributions, so that the relevant dynamical and non-dynamical correlation effects are properly coupled, is a useful feature too. Last but not least, the definition of the triply excited cluster amplitudes $t_{\underline{abc}}^{ijk}$, Eq. (8), adopted by the CCSDt philosophy guarantees systematic convergence toward the full treatment of triples as N_o and N_u approach n_o and n_u , respectively.

All of this suggests that one should be able to efficiently incorporate the connected triply excited clusters in the ACP considerations by replacing the CCSDt amplitude equations,

$$\langle \Phi_i^a | [H_N(1 + T_1 + T_2 + \frac{1}{2}T_1^2 + \mathbf{t}_3 + T_1 T_2 + \frac{1}{6}T_1^3)]_C | \Phi \rangle = 0, \quad (9)$$

$$\begin{aligned} \langle \Phi_{ij}^{ab} | [H_N(1 + T_1 + T_2 + \frac{1}{2}T_1^2 + \mathbf{t}_3 + T_1 T_2 + \frac{1}{6}T_1^3 + T_1 \mathbf{t}_3 + \frac{1}{2}T_1^2 T_2 + \frac{1}{24}T_1^4)]_C | \Phi \rangle \\ + \sum_{k=1}^5 \Lambda_k^{(2)}(ab, ij) = 0, \end{aligned} \quad (10)$$

$$\begin{aligned} \langle \Phi_{ij\mathbf{k}}^{abc} | [H_N(T_2 + \mathbf{t}_3 + T_1 T_2 + T_1 \mathbf{t}_3 + \frac{1}{2}T_2^2 + \frac{1}{2}T_1^2 T_2 \\ + T_2 \mathbf{t}_3 + \frac{1}{2}T_1^2 \mathbf{t}_3 + \frac{1}{2}T_1 T_2^2 + \frac{1}{6}T_1^3 T_2)]_C | \Phi \rangle = 0, \end{aligned} \quad (11)$$

where $|\Phi_i^a\rangle$ and $|\Phi_{ij}^{ab}\rangle$ are the singly and doubly excited determinants, $|\Phi_{ij\mathbf{k}}^{abc}\rangle$ are the selected triply excited determinants entering the definition of \mathbf{t}_3 , Eq. (8), and $\Lambda_k^{(2)}(ab, ij)$, $k = 1-5$, are the five Goldstone–Hugenholtz diagrammatic contributions to the $\langle \Phi_{ij}^{ab} | (H_N \frac{1}{2}T_2^2)_C | \Phi \rangle$ term in the equations projected on the doubly excited determinants, by their ACCSDt counterparts, in which we replace Eq. (10) in the above system by

$$\begin{aligned} \langle \Phi_{ij}^{ab} | [H_N(1 + T_1 + T_2 + \frac{1}{2}T_1^2 + \mathbf{t}_3 + T_1 T_2 + \frac{1}{6}T_1^3 + T_1 \mathbf{t}_3 + \frac{1}{2}T_1^2 T_2 + \frac{1}{24}T_1^4)]_C | \Phi \rangle \\ + \Lambda_1^{(2)}(ab, ij) + \lambda \Lambda_3^{(2)}(ab, ij) + (1 - \lambda) \Lambda_4^{(2)}(ab, ij) = 0. \end{aligned} \quad (12)$$

As already alluded to above, in this study we focus on the ACCSDt($1, 3 \times \frac{n_o}{n_o+n_u} + 4 \times \frac{n_u}{n_o+n_u}$) approach, in which λ in Eq. (12) is set at $\frac{n_o}{n_o+n_u}$, and its performance in the strongly correlated situations created by the H_6 and H_{10} rings and the H_{50} linear chain, for which the exact, FCI, or nearly exact, DMRG, data are available, although the closely related ACCSDt(1,3), ACCSDt(1,4), and ACCSDt($1, \frac{3+4}{2}$) schemes corresponding to $\lambda = 1, 0$, and $\frac{1}{2}$, respectively, are considered in our calculations as well. Along with the ACCSDt($1, 3 \times \frac{n_o}{n_o+n_u} + 4 \times \frac{n_u}{n_o+n_u}$), ACCSDt(1,3), ACCSDt(1,4), and ACCSDt($1, \frac{3+4}{2}$) methods, we examine their ACCSDT($1, 3 \times \frac{n_o}{n_o+n_u} + 4 \times \frac{n_u}{n_o+n_u}$), ACCSDT(1,3), ACCSDT(1,4), and ACCSDT($1, \frac{3+4}{2}$) parents, which are obtained by replacing \mathbf{t}_3 in Eqs. (9), (11), and (12) by its T_3 counterpart, *i.e.*, by making all orbitals used to define the triply excited amplitudes and determinants active. Unlike in Refs. [147, 148, 151, 159, 160], where the authors were primarily interested in retaining the exactness for three-electron systems, we do not attempt to alter or simplify the amplitude equations corresponding to the projections on the triply excited determinants in our ACCSDt and ACCSDT schemes. Our main interest in this exploratory study is the examination of a strongly correlated regime of the type of metal-insulator transitions modeled by the dissociating hydrogen rings and linear chains, and model systems that were used in the past to advocate diagram cancellations in similar situations, including the aforementioned cyclic polyenes in the Hubbard and PPP Hamiltonian description, do not provide any specific guidance how to handle the connected triply excited clusters. Thus, as shown in Eq. (11), we keep all terms in the CC equations projected on the triply excited determinants resulting from the use of the exponential wave function ansatz in which the cluster operator T is truncated at the three-body component, and then, whenever possible, *i.e.*, when the basis set used in the calculations is larger than a minimum one, reduce the computational costs associated with the full treatment of T_3 by constraining the indices in the t_{abc}^{ijk} amplitudes following the CCSDt recipe defined by Eq. (8).

C. Computational Details

All of the triples-corrected ACP methods discussed in Section II B, which emerge from replacing Eq. (10) in the CCSDt/CCSDT system by Eq. (12) with the appropriate λ values, including ACCSDt($1, 3 \times \frac{n_o}{n_o+n_u} + 4 \times \frac{n_u}{n_o+n_u}$), ACCSDt(1,3), ACCSDt(1,4), and ACCSDt($1, \frac{3+4}{2}$), where the connected triply excited clusters are treated using active orbitals, and their respec-

tive ACCSDT($1, 3 \times \frac{n_o}{n_o+n_u} + 4 \times \frac{n_u}{n_o+n_u}$), ACCSDT(1,3), ACCSDT(1,4), and ACCSDT($1, \frac{3+4}{2}$) parents, in which T_3 clusters are treated fully, have been implemented in our local version of the GAMESS package [210–212]. The resulting codes, which work with the RHF as well as restricted open-shell Hartree–Fock references, and the analogous computer programs that enable the ACCSD($1, 3 \times \frac{n_o}{n_o+n_u} + 4 \times \frac{n_u}{n_o+n_u}$), ACCSD(1,3), ACCSD(1,4), and ACCSD($1, \frac{3+4}{2}$) = DCSD calculations, in which the connected triply excited clusters are neglected, have been generated by making suitable modifications in our previously developed [213–216] CCSD, CCSDt, and CCSDT GAMESS routines. As in the case of other CC methodologies pursued by our group in the past (*cf.* Section III.B in Ref. [212] for the relevant information), our plan is to make all of the above ACP schemes, with and without connected triples, available in the official GAMESS distribution.

In order to test the performance of the ACP methods implemented in this work, especially the benefits offered by the active-space ACCSDt($1, 3 \times \frac{n_o}{n_o+n_u} + 4 \times \frac{n_u}{n_o+n_u}$) scheme and its ACCSDT($1, 3 \times \frac{n_o}{n_o+n_u} + 4 \times \frac{n_u}{n_o+n_u}$) parent compared to the remaining ACCSDt and ACCSDT approaches discussed in Section II B and the underlying ACCSD approximations in a strongly correlated regime, we carried out a series of calculations for the symmetric dissociations of the H_6 and H_{10} rings and the H_{50} linear chain, for which the conventional CCSD, CCSDt, and CCSDT methods fail as the H–H distances simultaneously increase. In the case of the D_{6h} -symmetric H_6 and D_{10h} -symmetric H_{10} ring systems, we employed the largest basis sets that allowed us to perform the exact, FCI, computations using the determinantal FCI code [106, 107, 217] available in GAMESS. Those were the polarized valence correlation-consistent basis set of the triple- ζ quality using spherical d functions, commonly abbreviated as cc-pVTZ [218], for H_6 , which results in the many-electron Hilbert space spanned by $\sim 10^9$ singlet CSFs, and the double- ζ (DZ) basis of Refs. [219, 220] in the case of H_{10} , giving rise to a FCI problem on the order of 10^7 singlet CSFs (we could not use basis sets of the triple- ζ quality or a DZ basis augmented with polarization functions in the latter case, since the resulting Hamiltonian diagonalizations using the FCI algorithms available in GAMESS turned out to be prohibitively expensive for us). In addition to illustrating the computational efficiency of our active-space ACCSDt schemes compared to their ACCSDT counterparts, the use of basis sets larger than a minimum one for the H_6 and H_{10} systems allows us to demonstrate that scaling diagrams (3) and (4) in ACCSDt($1, 3 \times \frac{n_o}{n_o+n_u} + 4 \times \frac{n_u}{n_o+n_u}$) and ACCSDT($1, 3 \times \frac{n_o}{n_o+n_u} + 4 \times \frac{n_u}{n_o+n_u}$) with factors depending on the numbers of occupied and

unoccupied orbitals involved in the calculations can benefit the resulting energetics. When considering the symmetric dissociation of the equidistant H_{50} linear chain, we had to proceed differently. In this case, the exact Hamiltonian diagonalization becomes prohibitively expensive even when a minimum basis set is employed (when $n_o = n_u = 25$, one already needs $\sim 10^{27}$ singlet CSFs to define the corresponding many-electron Hilbert space). Thus, in applying the ACP approaches examined in this study to the H_{50} linear chain, we relied on the nearly exact results reported for this system in Ref. [47], which were obtained with the DMRG algorithm abbreviated as LDMRG(500) and the STO-6G minimum basis set [221]. All of the CC (CCSD, CCSDt, and CCSDT) and ACP (ACCSd, ACCSDt, and ACCSDT) calculations reported in this article employed the RHF determinant as a reference.

In line with the nature of strong correlations created by the dissociations of the above hydrogen clusters, the active orbitals used in the ACCSDt and CCSDt calculations consisted of the molecular orbitals (MOs) that correlate with the $1s$ shells of the hydrogen atoms. This means that the ACCSDt and CCSDt computations for the H_6 ring were performed using three active occupied and three active unoccupied orbitals ($N_o = N_u = 3$), whereas the analogous calculations for the H_{10} system used five active occupied and five active unoccupied MOs ($N_o = N_u = 5$). Because of the use of the cc-pVTZ basis for H_6 and the DZ basis for H_{10} , *i.e.*, basis sets that are considerably larger than a minimum one, the numbers of active unoccupied orbitals used in the ACCSDt and CCSDt computations for the dissociating H_6 and H_{10} rings, especially for H_6 , were much smaller than the numbers of all unoccupied MOs characterizing these systems (81 and 15, respectively). In the case of the H_{50} linear chain, where, to be consistent with Ref. [47] that provided the LDMRG(500) reference data, we had to use the STO-6G minimum basis set, the only meaningful active space is that incorporating all 25 occupied and all 25 unoccupied orbitals. Thus, our ACCSDt and CCSDt results for this system are equivalent to those obtained in the respective ACCSDT and CCSDT calculations. Furthermore, since $n_o = n_u$ in this case and the differences between the $\text{ACCSdT}(1, 3 \times \frac{n_o}{n_o+n_u} + 4 \times \frac{n_u}{n_o+n_u}) = \text{ACCSdT}(1, \frac{3+4}{2})$, $\text{ACCSdT}(1,3)$, and $\text{ACCSdT}(1,4)$ energies for the H_{50} linear chain described by the STO-6G basis set are rather small (for each of the studied geometries, less than 1% of the correlation energy), in reporting our results for this system we focus on the $\text{ACCSdT}(1, \frac{3+4}{2})$ calculations and the associated $\text{ACCSd}(1, \frac{3+4}{2}) = \text{DCSD}$, CCSD, and CCSDT data.

All of the calculations for the symmetric dissociations of the H_6 and H_{10} rings reported in

this article employed the following grid of internuclear separations between the neighboring hydrogen atoms, denoted as $R_{\text{H-H}}$, to determine the corresponding potential energy curves (PECs): 0.6, 0.7, 0.8, 0.9, 1.0, 1.1, 1.2, 1.3, 1.4, 1.5, 1.6, 1.7, 1.8, 1.9, 2.0, 2.1, 2.2, 2.3, 2.4, and 2.5 Å. The PECs characterizing the symmetric dissociation of the H_{50} linear chain were calculated at the geometries defined by the $R_{\text{H-H}}$ values used in Ref. [47], namely, 1.0, 1.2, 1.4, 1.6, 1.8, 2.0, 2.4, 2.8, 3.2, and 3.6 bohr (the authors of Ref. [47] considered one additional H-H distance of 4.2 bohr, but we run into difficulties with converging our ACCSDT($1, \frac{3+4}{2}$) calculations in this case, so the largest H-H separation reported in this work is 3.6 bohr).

III. NUMERICAL RESULTS

A. Symmetric Dissociation of the H_6 and H_{10} Rings

We begin our discussion of the numerical results obtained in this work by examining the D_{6h} -symmetric dissociation of the six-membered hydrogen ring, as described by the cc-pVTZ basis set. The information about the ground-state PECs of the $\text{H}_6/\text{cc-pVTZ}$ system obtained in the conventional CCSD, CCSDt, and CCSDT calculations, their ACCSD, ACCSDt, and ACCSDT counterparts, and the exact FCI diagonalizations is summarized in Tables I–III and Fig. 2. Table I reports the results of the computations performed with the various CCSD-type levels, including CCSD, ACCSD(1,3), ACCSD($1, \frac{3+4}{2}$) = DCSD, ACCSD($1, 3 \times \frac{n_o}{n_o+n_u} + 4 \times \frac{n_u}{n_o+n_u}$), and ACCSD(1,4). The analogous results obtained with the CCSDt-type methods, which describe the effects of T_3 correlations with the help of active orbitals, including CCSDt, ACCSDt(1,3), ACCSDt($1, \frac{3+4}{2}$), ACCSDt($1, 3 \times \frac{n_o}{n_o+n_u} + 4 \times \frac{n_u}{n_o+n_u}$), and ACCSDt(1,4), are shown in Table II. Table III summarizes the calculations carried out with the CCSDT, ACCSDT(1,3), ACCSDT($1, \frac{3+4}{2}$), ACCSDT($1, 3 \times \frac{n_o}{n_o+n_u} + 4 \times \frac{n_u}{n_o+n_u}$), and ACCSDT(1,4), approaches, in which T_3 clusters are treated fully. As already alluded to above, because of the use of the cc-pVTZ basis set in our calculations for the hexagonal H_6 system, the dimension of the corresponding many-electron Hilbert space is on the order of 10^9 (in our FCI calculations employing the determinantal GAMESS routines that permit the use of Abelian symmetries, the number of determinants relevant to the exact ground-state problem, *i.e.*, the $S_z = 0$ determinants belonging to the A_g irreducible representation of the largest Abelian subgroup of D_{6h} , which is D_{2h} , was 1,139,812,264). The ACCSD($1, \frac{3+4}{2}$) =

DCSD calculations for the symmetric dissociation of the H_6 ring system were also reported in Ref. [52], but, unlike in the present study, the authors of Ref. [52] used a minimum basis set, which results in the many-electron Hilbert space 7 orders of magnitude smaller than that generated with cc-pVTZ, and did not consider the effects of T_3 correlations on the resulting PEC. It is, therefore, interesting to examine how the use of a much larger cc-pVTZ basis and the incorporation of the connected triply excited clusters in the calculations affects the observations made in Ref. [52]. It is also worth investigating if the replacement of the ACCSDT($1, \frac{3+4}{2}$) scheme and its active-space ACCSDt($1, \frac{3+4}{2}$) counterpart, which build upon DCSD, by the ACCSDT($1, 3 \times \frac{n_o}{n_o+n_u} + 4 \times \frac{n_u}{n_o+n_u}$) and ACCSDt($1, 3 \times \frac{n_o}{n_o+n_u} + 4 \times \frac{n_u}{n_o+n_u}$) approaches proposed in this work provides improvements over the results of the analogous ACCSDT($1, \frac{3+4}{2}$) and ACCSDt($1, \frac{3+4}{2}$) calculations.

As shown in Tables I–III and Fig. 2, the conventional CCSD, CCSDt, and CCSDT methods applied to the symmetric dissociation of the H_6 /cc-pVTZ ring system fail when the strongly correlated region of larger H–H separations is considered. In fact, they break down rather quickly as the R_{H-H} values increase. This can be illustrated by the very large negative errors relative to FCI resulting from the CCSD, CCSDt, and CCSDT calculations in the $R_{H-H} \geq 2.0$ Å region, which grow, in absolute value, from about 25–35 mE_h at $R_{H-H} = 2.0$ Å to gargantuan 237–246 mE_h when the distance between the neighboring H–H atoms in the hexagonal H_6 system reaches 2.5 Å. All three CC approaches produce completely erratic, similarly shaped, PECs, with an unphysical hump at the intermediate stretches of the H–H bonds and a well-displayed downhill behavior as the R_{H-H} values approach the strongly correlated asymptotic region. As one might have anticipated based on the examination of strongly correlated model systems [67, 117, 118] (*cf.*, also, Refs. [63, 65]), the explicit inclusion of the connected triply excited clusters through the full CCSDT treatment and its active-space CCSDt counterpart offers no help in this regard. The CCSDt and CCSDT approaches improve the CCSD results in the weakly correlated equilibrium region, reducing the 4.424 mE_h error relative to FCI obtained with CCSD at $R_{H-H} = 1.0$ Å to 1.804 mE_h and 0.160 mE_h, respectively, but they are as inaccurate as CCSD (or even less accurate) when the H–H distances become larger. The only benefit of using CCSDt is a major reduction in the computational timings compared to CCSDT, from 98 s per iteration in the latter case to 6 s per iteration in the case of the former method (timings obtained using a single core of the Precision 7920 system from Dell equipped with 10-core Intel Xeon Silver 4114 2.2 GHz

processor boards), with minimum loss of accuracy, especially at larger H–H separations, but the fact that the CCSDt approach faithfully reproduces the CCSDT PEC at the small fraction of the effort is of no help here, since both PECs are qualitatively incorrect.

A quick inspection of Fig. 2 reveals that all ACP methods examined in this study, without and with the connected triples, provide qualitatively correct PECs for the D_{6h} -symmetric dissociation of the H_6/cc -pVTZ ring. As demonstrated in Tables I–III and Fig. 2, they eliminate the erratic behavior of the conventional CCSD, CCSDt, and CCSDT approaches in a strongly correlated regime, while producing the energies that remain close to those obtained with FCI at all H–H separations considered in our calculations. Focusing first on the ACP methodologies with up to two-body clusters, meaning ACCSD(1,3), $ACCSD(1, \frac{3+4}{2}) = DCSD$, $ACCSD(1, 3 \times \frac{n_o}{n_o+n_u} + 4 \times \frac{n_u}{n_o+n_u})$, and ACCSD(1,4), the ACCSD(1,3) scheme, which corresponds to setting λ in Eqs. (6) and (12) at 1, performs the best, generating a PEC that closely reproduces its exact, FCI, counterpart. This can be illustrated by the small mean unsigned error (MUE) and mean signed error (MSE) values relative to FCI characterizing the ACCSD(1,3) PEC, which are 0.675 mE_h and −0.311 mE_h, respectively (see Table I). The ACCSD approach at the other end of the spectrum, *i.e.*, ACCSD(1,4), which is obtained by using $\lambda = 0$ in Eqs. (6) and (12), while being qualitatively correct, does not work as well as its ACCSD(1,3) counterpart, increasing the MUE and MSE values relative to FCI to more than 9 mE_h. As a result, the $ACCSD(1, \frac{3+4}{2}) = DCSD$ method, which treats diagrams (3) and (4) shown Fig. 1 on equal footing by setting λ in Eqs. (6) and (12) at $\frac{1}{2}$, produces a PEC that is more or less the average of the PECs obtained in the ACCSD(1,3) and ACCSD(1,4) calculations [see panels (a) and (d) of Fig. 2 and Table I]. This should be contrasted by the $ACCSD(1, 3 \times \frac{n_o}{n_o+n_u} + 4 \times \frac{n_u}{n_o+n_u})$ computations, in which λ in Eqs. (6) and (12) is set at $\frac{n_o}{n_o+n_u}$ and which result in a PEC similar to that obtained with the ACCSD(1,4) approach, improving the ACCSD(1,4) energetics only slightly. This behavior of the $ACCSD(1, 3 \times \frac{n_o}{n_o+n_u} + 4 \times \frac{n_u}{n_o+n_u})$ method can be understood if we realize that the numbers of occupied and unoccupied orbitals involved in the calculations for the H_6/cc -pVTZ system are 3 and 81, respectively, so that $n_u = 27n_o \gg n_o$, making the scaling factors at diagrams (3) and (4) in Eqs. (6) and (12) close to 0 and 1, respectively, and the $ACCSD(1, 3 \times \frac{n_o}{n_o+n_u} + 4 \times \frac{n_u}{n_o+n_u})$ approach similar to ACCSD(1,4).

Based on the above discussion, one might crown the ACCSD(1,3) scheme the best ACP approach examined in the present study, but this would be misleading. Given the to-

tal neglect of T_3 correlations in the ACCSD(1,3) (and all other ACCSD) calculations, the excellent performance of the ACCSD(1,3) method in reproducing the FCI energetics characterizing the metal–insulator transition in the hexagonal H_6 /cc-pVTZ system discussed here is fortuitous. As explained in Section II A, the ACP approaches can be very effective in capturing the non-dynamical correlation effects associated with the entanglement of larger numbers of electrons by taking advantage of the cancellations of certain $(T_2)^2$ diagrams in the CCD/CCSD equations projected on the doubly excited CSFs or determinants in a strongly correlated regime modeled by the Hubbard and PPP Hamiltonians. However, as pointed out above, in Section II A as well, the diagram cancellations within the CCD/CCSD amplitude equations that result in the ACP methods of the ACCSD(1,3), ACCSD(1,4), or ACCSD($1, \frac{3+4}{2}$) = DCSD type do not describe the T_3 physics needed to capture much of the remaining dynamical and non-dynamical correlations and obtain a quantitative description of realistic systems described by *ab initio* Hamiltonians. It is, therefore, essential to examine what happens when the various ACCSD approaches considered in this study are embedded in the CCSDt/CCSDT amplitude equations following the recipe discussed in Section II B.

As shown in Tables II and III and panels (b), (c), (e), and (f) in Fig. 2, the inclusion of the connected triply excited clusters in the ACP schemes, following the procedure described by Eqs. (9), (11), and (12), has interesting effects on the ACCSD(1,3), ACCSD($1, \frac{3+4}{2}$) = DCSD, ACCSD($1, 3 \times \frac{n_o}{n_o+n_u} + 4 \times \frac{n_u}{n_o+n_u}$), and ACCSD(1,4) energetics. The selection of the $(T_2)^2$ diagrams (1) and (3) of Fig. 1, which produced the most accurate PEC for the symmetric dissociation of the H_6 /cc-pVTZ system among the various ACCSD methods considered in this work, results in the worst description when the ACCSDT(1,3), ACCSDT($1, \frac{3+4}{2}$), ACCSDT($1, 3 \times \frac{n_o}{n_o+n_u} + 4 \times \frac{n_u}{n_o+n_u}$), and ACCSDT(1,4) PECs and their analogs obtained in the active-space ACCSDt(1,3), ACCSDt($1, \frac{3+4}{2}$), ACCSDt($1, 3 \times \frac{n_o}{n_o+n_u} + 4 \times \frac{n_u}{n_o+n_u}$), and ACCSDt(1,4) calculations are compared with one another. To make matters worse, the ACCSDt(1,3) and ACCSDT(1,3) approaches, in spite of accounting for T_3 correlations, are considerably less accurate than their ACCSD(1,3) counterpart, in which the connected triple excitations are ignored. This is in sharp contrast with the remaining ACCSDt and ACCSDT methods considered in this study, which all improve the underlying ACCSD results. There is, however, a significant difference between the ACCSDT($1, 3 \times \frac{n_o}{n_o+n_u} + 4 \times \frac{n_u}{n_o+n_u}$) and ACCSDT(1,4) approaches and their active-space ACCSDt($1, 3 \times \frac{n_o}{n_o+n_u} + 4 \times \frac{n_u}{n_o+n_u}$) and ACCSDt(1,4) counterparts, which are obtained by including the connected triply excited

clusters on top of ACCSD($1, 3 \times \frac{n_o}{n_o+n_u} + 4 \times \frac{n_u}{n_o+n_u}$) and ACCSD(1,4), respectively, and the ACCSDT($1, \frac{3+4}{2}$) and ACCSDt($1, \frac{3+4}{2}$) approximations that build upon ACCSD($1, \frac{3+4}{2}$) = DCSD. The ACCSD(1,4), ACCSDt(1,4), and ACCSDT(1,4) methods form a systematically improvable hierarchy, with the MUE values relative to FCI decreasing from 9.349 mE_h in the case of ACCSD(1,4) to 2.129 mE_h, when the ACCSDt(1,4) approximation to ACCSDT(1,4) is employed, and to 1.304 mE_h in the ACCSDT(1,4) case. The ACCSD($1, 3 \times \frac{n_o}{n_o+n_u} + 4 \times \frac{n_u}{n_o+n_u}$), ACCSDt($1, 3 \times \frac{n_o}{n_o+n_u} + 4 \times \frac{n_u}{n_o+n_u}$), and ACCSDT($1, 3 \times \frac{n_o}{n_o+n_u} + 4 \times \frac{n_u}{n_o+n_u}$) approaches behave in a similar manner, with the corresponding MUE values relative to FCI decreasing from 9.037 mE_h to 1.818 mE_h and 1.150 mE_h, respectively, further improving the ACCSDt(1,4) and ACCSDT(1,4) results, but the analogous DCSD-based sequence, *i.e.*, ACCSD($1, \frac{3+4}{2}$) = DCSD, ACCSDt($1, \frac{3+4}{2}$), and ACCSDT($1, \frac{3+4}{2}$), is no longer as systematic. Indeed, while the ACCSDt($1, \frac{3+4}{2}$) and ACCSDT($1, \frac{3+4}{2}$) calculations that include information about T_3 clusters are more accurate than their ACCSD($1, \frac{3+4}{2}$) counterpart, in which the effects of connected triples are neglected, the improvements offered by the ACCSDt($1, \frac{3+4}{2}$) and ACCSDT($1, \frac{3+4}{2}$) methods compared to ACCSD($1, \frac{3+4}{2}$) are rather small, reducing the MUE value relative to FCI characterizing the ACCSD($1, \frac{3+4}{2}$) calculations, of 4.770 mE_h, to 2.585 mE_h and 3.486 mE_h, respectively. Furthermore, unlike in the ACCSDt(1,4) *vs.* ACCSDT(1,4) and ACCSDt($1, 3 \times \frac{n_o}{n_o+n_u} + 4 \times \frac{n_u}{n_o+n_u}$) *vs.* ACCSDT($1, 3 \times \frac{n_o}{n_o+n_u} + 4 \times \frac{n_u}{n_o+n_u}$) computations, we do not observe improvements in the results, when the active-space ACCSDt($1, \frac{3+4}{2}$) approach is replaced by its ACCSDT($1, \frac{3+4}{2}$) parent. One should always observe improvements, when going from the CCSDt-level using small numbers of active orbitals to its CCSDT-type counterpart in larger basis set calculations, but this is not the case when the PECs describing the symmetric dissociation of the H₆/cc-pVTZ system obtained with the ACCSDt($1, \frac{3+4}{2}$) and ACCSDT($1, \frac{3+4}{2}$) methods are compared with each other. The ACCSDt(1,4)/ACCSDT(1,4) and, especially, the ACCSDt($1, 3 \times \frac{n_o}{n_o+n_u} + 4 \times \frac{n_u}{n_o+n_u}$)/ACCSDT($1, 3 \times \frac{n_o}{n_o+n_u} + 4 \times \frac{n_u}{n_o+n_u}$) pairs behave more systematically in this regard.

It is clear from the results presented in Tables II and III and panels (b), (c), (e), and (f) of Fig. 2 that from all T_3 -corrected CC and ACP methods investigated in this study, the ACCSDt($1, 3 \times \frac{n_o}{n_o+n_u} + 4 \times \frac{n_u}{n_o+n_u}$) and ACCSDT($1, 3 \times \frac{n_o}{n_o+n_u} + 4 \times \frac{n_u}{n_o+n_u}$) approaches provide the most accurate description of the dissociating H₆/cc-pVTZ ring that undergoes a transition from the weakly correlated metallic phase near the equilibrium geometry to the strongly correlated insulator at larger values of $R_{\text{H-H}}$. They eliminate dramatic failures of

CCSDt and CCSDT at larger H–H separations, they significantly improve the underlying ACCSD($1, 3 \times \frac{n_o}{n_o+n_u} + 4 \times \frac{n_u}{n_o+n_u}$) PEC, and they offer impressive, millihartree-type, accuracies in the entire region of the $R_{\text{H-H}}$ values examined in this work, recovering 99–100 % of the FCI correlation energy independent of $R_{\text{H-H}}$. It is also encouraging to observe that the n_o - and n_u -dependent diagram scaling factors adopted in the ACCSDt($1, 3 \times \frac{n_o}{n_o+n_u} + 4 \times \frac{n_u}{n_o+n_u}$) and ACCSDT($1, 3 \times \frac{n_o}{n_o+n_u} + 4 \times \frac{n_u}{n_o+n_u}$) schemes improve the ACCSDt($1, \frac{3+4}{2}$) and ACCSDT($1, \frac{3+4}{2}$) results and their ACCSDt(1,3)/ACCSDT(1,3) and ACCSDt(1,4)/ACCSDT(1,4) counterparts. To appreciate the significance of these findings even more, one should point out that the costs of the ACCSDt($1, 3 \times \frac{n_o}{n_o+n_u} + 4 \times \frac{n_u}{n_o+n_u}$) computations for the $\text{H}_6/\text{cc-pVTZ}$ system are not much greater than those characterizing the CCSD and ACCSD approximations. Indeed, we needed 2 s per iteration on a single core of the aforementioned Dell architecture to perform the CCSD or ACCSD calculations, which should be compared to 6 s required by the corresponding ACCSDt($1, 3 \times \frac{n_o}{n_o+n_u} + 4 \times \frac{n_u}{n_o+n_u}$) runs. The ACCSDT($1, 3 \times \frac{n_o}{n_o+n_u} + 4 \times \frac{n_u}{n_o+n_u}$) method, which offers a full treatment of T_3 correlations, improving the already excellent ACCSDt($1, 3 \times \frac{n_o}{n_o+n_u} + 4 \times \frac{n_u}{n_o+n_u}$) PEC even further, offers promise too. Obviously, the ACCSDT($1, 3 \times \frac{n_o}{n_o+n_u} + 4 \times \frac{n_u}{n_o+n_u}$) approach, using all triply excited cluster amplitudes, is less practical than its active-space ACCSDt($1, 3 \times \frac{n_o}{n_o+n_u} + 4 \times \frac{n_u}{n_o+n_u}$) counterpart, which uses their small fraction, but with less than 100 s per iteration on a single core of Dell machine used in our computations for the $\text{H}_6/\text{cc-pVTZ}$ system, it is orders of magnitude less expensive than the exact Hamiltonian diagonalizations, while providing similar results. Indeed, our FCI calculations for the $\text{H}_6/\text{cc-pVTZ}$ system required more than 7 h per iteration on the same core, even though they exploited the D_{2h} symmetry that was not used in our CC and ACP runs. Having said all this, the most important finding of our calculations for the symmetric dissociation of the $\text{H}_6/\text{cc-pVTZ}$ ring is the observation that the active-space ACCSDt($1, 3 \times \frac{n_o}{n_o+n_u} + 4 \times \frac{n_u}{n_o+n_u}$) approach provides the results of the near-FCI quality, capturing virtually all of the relevant dynamical and non-dynamical correlations, even at larger H–H separations, faithfully reproducing the accurate parent ACCSDT($1, 3 \times \frac{n_o}{n_o+n_u} + 4 \times \frac{n_u}{n_o+n_u}$) data at the small fraction of the computational cost, and reducing the timings of the exact Hamiltonian diagonalizations from hours per iteration to seconds.

To further investigate the performance of the ACP methods, especially those that incorporate T_3 physics, in a strongly correlated regime coupled with non-trivial dynamical correlations, we studied the D_{10h} -symmetric dissociation of the H_{10} ring, as described by

the DZ basis set. The ground-state PECs of the H_{10} /DZ system resulting from the CCSD, CCSDt, and CCSDT calculations, the corresponding ACCSD, ACCSDt, and ACCSDT runs, and the exact FCI computations are shown in Tables IV–VI and Fig. 3. Table IV summarizes the various CCSD-type calculations, including CCSD, ACCSD(1,3), ACCSD($1, \frac{3+4}{2}$) = DCSD, ACCSD($1, 3 \times \frac{n_o}{n_o+n_u} + 4 \times \frac{n_u}{n_o+n_u}$), and ACCSD(1,4). The results of the CCSDt, ACCSDt(1,3), ACCSDt($1, \frac{3+4}{2}$), ACCSDt($1, 3 \times \frac{n_o}{n_o+n_u} + 4 \times \frac{n_u}{n_o+n_u}$), and ACCSDt(1,4) computations are shown in Table V. The CCSDT, ACCSDT(1,3), ACCSDT($1, \frac{3+4}{2}$), ACCSDT($1, 3 \times \frac{n_o}{n_o+n_u} + 4 \times \frac{n_u}{n_o+n_u}$), and ACCSDT(1,4) calculations are summarized in Table VI.

The symmetric dissociation of the H_{10} system is more challenging than the previously discussed H_6 ring, since the ground electronic state of H_{10} , when all H–H distances are simultaneously stretched, involves the entanglement of 10 electrons, which is an increase in the number of strongly correlated electrons by two thirds. Because of the use of a smaller basis set, the dimension of the many-electron Hilbert space characterizing the D_{10h} -symmetric H_{10} /DZ system is smaller compared to H_6 using the cc-pVTZ basis [the number of the $S_z = 0$ determinants of the $A_g(D_{2h})$ symmetry used in our FCI GAMESS calculations for the H_{10} /DZ system was 60,095,104, as opposed to 1,139,812,264 used for H_6 /cc-pVTZ], but the challenge of strong correlations created by the simultaneous dissociation of all H–H bonds in the H_{10} ring is more severe than in the case of its hexagonal H_6 cousin. This can be seen when examining the performance of the CCSD, CCSDt, and CCSDT approaches. As shown in Tables IV–VI and Fig. 3, the PECs resulting from the CCSD, CCSDt, and CCSDT calculations are not only incorrectly shaped, exhibiting an unphysical hump at the intermediate stretches of the H–H bonds, but they cannot be continued beyond $R_{H-H} \approx 1.7$ Å. The CCSDt and CCSDT methods reduce the ~ 4 – 7 mE_h errors relative to FCI obtained with the CCSD approach in the equilibrium ($R_{H-H} \approx 1.0$ Å) region to small fractions of a millihartree, but when $R_{H-H} > 1.7$ Å, the CCSD, CCSDt, and CCSDT calculations diverge, even when initiated from the converged cluster amplitudes obtained at the neighboring geometries from the $R_{H-H} \leq 1.7$ Å region. As argued in Refs. [60, 63], using detailed mathematical analysis of the analytic properties of non-linear CC equations and the relevant numerical evidence, this is, most likely, caused by the existence of branch point singularities in the vicinity of the $R_{H-H} \approx 1.7$ Å geometry and the CCSD, CCSDt, and CCSDT solutions becoming complex when $R_{H-H} > 1.7$ Å. The singularities and divergences of this kind were observed in the conventional CC calculations for the cyclic polyene models with 14 or more carbon sites

[60–67], and we believe that our CCSD, CCSDt, and CCSDT computations for the D_{10h} -symmetric dissociation of the H_{10} ring suffer from similar problems once the region of larger H–H separations is reached.

Tables IV–VI and Fig. 3 demonstrate that all ACP methods investigated in this work are capable of eliminating the singular behavior observed in the CCSD, CCSDt, and CCSDT calculations for the dissociating H_{10} system. As was the case with the smaller H_6 ring, the ACCSD(1,3), $\text{ACCSD}(1, \frac{3+4}{2}) = \text{DCSD}$, $\text{ACCSD}(1, 3 \times \frac{n_o}{n_o+n_u} + 4 \times \frac{n_u}{n_o+n_u})$, and ACCSD(1,4) approaches and their ACCSDt and ACCSDT counterparts produce the qualitatively correct PECs that are in reasonable agreement with FCI, even when the H–H bonds in H_{10} are significantly stretched. Although the DZ basis set used in our calculations for the H_{10} system, in which $n_o = 5$ and $n_u = 15$, is much smaller than the cc-pVTZ basis used in the case of H_6 , many of the accuracy patterns observed in the ACP computations for the H_6 ring apply to the symmetric dissociation of its ten-membered analog. For example, among the ACP schemes truncated at T_2 examined in this study, the ACCSD(1,3) method is most accurate and the ACCSD(1,4) approach performs worst, increasing the MUE and MSE values relative to FCI obtained with ACCSD(1,3), of 12.572 mE_h, to 15.505 mE_h [see Table IV and panels (a) and (d) in Fig. 3]. In analogy to the hexagonal H_6 system, the $\text{ACCSD}(1, \frac{3+4}{2}) = \text{DCSD}$ and $\text{ACCSD}(1, 3 \times \frac{n_o}{n_o+n_u} + 4 \times \frac{n_u}{n_o+n_u})$ methods, which average the contributions from diagrams (3) and (4) of Fig. 1, produce the PECs located between the ACCSD(1,3) and ACCSD(1,4) ones. The $\text{ACCSD}(1, 3 \times \frac{n_o}{n_o+n_u} + 4 \times \frac{n_u}{n_o+n_u})$ PEC is closer to that obtained in the ACCSD(1,4) calculations, since the λ factor entering Eqs. (6) and (12) used by ACCSD(1, $\frac{3+4}{2}$) is $\frac{1}{2}$, whereas the $\text{ACCSD}(1, 3 \times \frac{n_o}{n_o+n_u} + 4 \times \frac{n_u}{n_o+n_u})$ approach proposed in this work adopts the weighted average defined by $\lambda = \frac{n_o}{n_o+n_u}$, which in the case of the H_{10}/DZ system considered here corresponds to setting λ at $\frac{1}{4}$, increasing the relative contribution of diagram (4) in Eqs. (6) and (12). Compared to the $H_6/\text{cc-pVTZ}$ system, the differences among the ACCSD(1,3), $\text{ACCSD}(1, \frac{3+4}{2})$, $\text{ACCSD}(1, 3 \times \frac{n_o}{n_o+n_u} + 4 \times \frac{n_u}{n_o+n_u})$, and ACCSD(1,4) PECs corresponding to the symmetric dissociation of the H_{10} ring are smaller, which is a consequence of the use of a smaller DZ basis set in the latter case [in the extreme limit of a minimum basis, where the p–h symmetry is approximately satisfied, the ACCSD(1,3), $\text{ACCSD}(1, \frac{3+4}{2})$, $\text{ACCSD}(1, 3 \times \frac{n_o}{n_o+n_u} + 4 \times \frac{n_u}{n_o+n_u})$, and ACCSD(1,4) results would be virtually identical], but the overall accuracy patterns characterizing the ACP methods with up to two-body clusters, especially the superior performance of the ACCSD(1,3) approximation, hold.

Because of the use of a smaller DZ basis in our calculations for the H_{10} system, the similarities in the performance of the ACP methods using different ways of mixing diagrams (3) and (4) in Eqs. (6) and (12) are also observed at the ACCSDt and ACCSDT levels, but, as shown in Tables V and VI and panels (b), (c), (e), and (f) of Fig. 3, the PECs resulting from the $\text{ACCSDt}(1, 3 \times \frac{n_o}{n_o+n_u} + 4 \times \frac{n_u}{n_o+n_u})$ and $\text{ACCSDT}(1, 3 \times \frac{n_o}{n_o+n_u} + 4 \times \frac{n_u}{n_o+n_u})$ calculations are most accurate when the H–H distances are larger. All of the ACP approaches with the connected triply excited clusters examined in this work, including $\text{ACCSDT}(1, 3)$, $\text{ACCSDT}(1, \frac{3+4}{2})$, $\text{ACCSDT}(1, 3 \times \frac{n_o}{n_o+n_u} + 4 \times \frac{n_u}{n_o+n_u})$, and $\text{ACCSDT}(1, 4)$ and their active-space $\text{ACCSDt}(1, 3)$, $\text{ACCSDt}(1, \frac{3+4}{2})$, $\text{ACCSDt}(1, 3 \times \frac{n_o}{n_o+n_u} + 4 \times \frac{n_u}{n_o+n_u})$, and $\text{ACCSDt}(1, 4)$ counterparts, offer major improvements in the underlying $\text{ACCSD}(1, 3)$, $\text{ACCSD}(1, \frac{3+4}{2}) = \text{DCSD}$, $\text{ACCSD}(1, 3 \times \frac{n_o}{n_o+n_u} + 4 \times \frac{n_u}{n_o+n_u})$, and $\text{ACCSD}(1, 4)$ results, reducing the MUE and MSE values relative to FCI by factors of ~ 2 – 4 , but, as in the case of the symmetric dissociation of the H_6 ring, the $\text{ACCSDt}(1, 3 \times \frac{n_o}{n_o+n_u} + 4 \times \frac{n_u}{n_o+n_u})$ and $\text{ACCSDT}(1, 3 \times \frac{n_o}{n_o+n_u} + 4 \times \frac{n_u}{n_o+n_u})$ methods perform best overall. Independent of the H–H separation, including the $R_{\text{H-H}}$ values as large as 2.5 \AA (we recall that the equilibrium value of $R_{\text{H-H}}$ is about 1.0 \AA), they reproduce the FCI correlation energies to within 1–2 % or about 3.8–3.9 mE_h on average. If we limit ourselves to the $R_{\text{H-H}} = 0.6$ – 2.0 \AA region, the errors in the $\text{ACCSDt}(1, 3 \times \frac{n_o}{n_o+n_u} + 4 \times \frac{n_u}{n_o+n_u})$ and $\text{ACCSDT}(1, 3 \times \frac{n_o}{n_o+n_u} + 4 \times \frac{n_u}{n_o+n_u})$ energies relative to FCI are in the ~ 1 – 3 mE_h range. Given the dramatic failure and the singular behavior of the conventional CCSDt and CCSDT approaches and the MUE values characterizing the $\text{ACCSDt}(1, 3 \times \frac{n_o}{n_o+n_u} + 4 \times \frac{n_u}{n_o+n_u})$ and $\text{ACCSDT}(1, 3 \times \frac{n_o}{n_o+n_u} + 4 \times \frac{n_u}{n_o+n_u})$ calculations being 3–4 times smaller compared to $\text{ACCSD}(1, 3)$, $\text{ACCSD}(1, \frac{3+4}{2})$, $\text{ACCSD}(1, 3 \times \frac{n_o}{n_o+n_u} + 4 \times \frac{n_u}{n_o+n_u})$, and $\text{ACCSD}(1, 4)$, we are encouraged by the performance of the $\text{ACCSDt}(1, 3 \times \frac{n_o}{n_o+n_u} + 4 \times \frac{n_u}{n_o+n_u})$ and $\text{ACCSDT}(1, 3 \times \frac{n_o}{n_o+n_u} + 4 \times \frac{n_u}{n_o+n_u})$ schemes developed in this work. It is also encouraging that the unscaled $\text{ACCSDt}(1, 4)$ and $\text{ACCSDT}(1, 4)$ methods, which correspond to setting λ in Eqs. (6) and (12) at 0 and which build upon the old $\text{ACCSD}(1, 4)$ approximation proposed in Ref. [64] by incorporating T_3 correlations in it, are practically as accurate. In particular, they improve the results obtained with the $\text{ACCSDt}(1, \frac{3+4}{2})$ and $\text{ACCSDT}(1, \frac{3+4}{2})$ approaches, which extend the $\text{ACCSD}(1, \frac{3+4}{2}) = \text{DCSD}$ scheme to the CCSDt/CCSDT-type treatments of the connected triples.

Last but not least, our calculations for the symmetric dissociation of the H_{10} ring system summarized in Tables V and VI and panels (b), (c), (e), and (f) confirm the previous

observation that the active-space ACCSDt methods faithfully reproduce the corresponding ACCSDT energetics, even at larger H–H separations, at the small fraction of the computational cost. The differences between the ACCSDt(1,3), ACCSDt(1, $\frac{3+4}{2}$), ACCSDt(1, $3 \times \frac{n_o}{n_o+n_u} + 4 \times \frac{n_u}{n_o+n_u}$), and ACCSDt(1,4) results and their respective ACCSDT(1,3), ACCSDT(1, $\frac{3+4}{2}$), ACCSDT(1, $3 \times \frac{n_o}{n_o+n_u} + 4 \times \frac{n_u}{n_o+n_u}$), and ACCSDT(1,4) parents obtained for the H₁₀ system are smaller than in the case of the previously discussed H₆ ring, since the DZ basis set used in our calculations for H₁₀ is much smaller than the cc-pVTZ basis employed in the H₆ case and, as a consequence, the number of active unoccupied orbitals used in the ACCSDt calculations for the H₁₀/DZ system is a significant fraction (one third) of all unoccupied MOs, but we still see substantial reduction in the computational effort offered by the active-space treatment of triples compared to the corresponding ACCSDT levels, from 2 s per iteration on a single core of the aforementioned Dell node in the case of ACCSDT to 0.7 s in the ACCSDt case.

B. Symmetric Dissociation of the H₅₀ Linear Chain

Having analyzed the performance of the various ACP approaches, especially those incorporating the connected three-body clusters, in calculations for the symmetric dissociations of the six- and ten-membered hydrogen rings, we proceed to the examination of our final example, which is the H₅₀ linear chain. As in the case of the H₆ and H₁₀ systems discussed in Section III A, we model the transition from the weakly correlated metallic regime in the equilibrium region, where the distances between the adjacent hydrogen atoms are around 1.8 bohr, to the strongly correlated insulator phase by simultaneously stretching all H–H bonds. Putting aside the periodic nature of the H₆ and H₁₀ ring structures, the main difference between the H₆ and H₁₀ clusters and the H₅₀ linear chain is a much larger number of the strongly correlated electrons in the latter system, which results in an enormous many-electron Hilbert space, spanned by $\sim 10^{27}$ singlet CSFs when the minimum basis set is employed and even larger numbers of CSFs when larger basis sets are considered. As already alluded to above, the exact Hamiltonian diagonalizations for the many-electron Hilbert spaces of such dimensionalities are outside reach of the best FCI algorithms and most powerful computer architectures available today, so in evaluating the performance of the ACP approaches considered in this work in calculations for the symmetric dissociation of the H₅₀

linear chain, we relied on the nearly exact PEC obtained in the LDMRG(500) computations using the STO-6G minimum basis set reported in Ref. [47]. Because of the use of the minimum basis, for which $n_o = n_u = N_o = N_u = 25$, our ACCSDt and CCSDt calculations for the H_{50} system are equivalent to their ACCSDT and CCSDT counterparts and the PECs obtained with the $\text{ACCSDT}(1, 3 \times \frac{n_o}{n_o+n_u} + 4 \times \frac{n_u}{n_o+n_u}) = \text{ACCSDT}(1, \frac{3+4}{2})$, $\text{ACCSDT}(1,3)$, and $\text{ACCSDT}(1,4)$ approaches are nearly identical, so in the discussion below we concentrate on the $\text{ACCSDT}(1, \frac{3+4}{2})$ results and the results generated with CCSD, CCSDT, and $\text{ACCSD}(1, \frac{3+4}{2}) = \text{DCSD}$. The DCSD calculations for the symmetric dissociation of the H_{50} linear chain, as described by the STO-6G basis set, were also reported in Ref. [52], but the authors of Ref. [52] did not consider T_3 correlations in their work. Our computations for the H_{50} /STO-6G system discussed in this section allow us to investigate if the inclusion of the connected triply excited clusters via the $\text{ACCSDT}(1, \frac{3+4}{2})$ scheme implemented in this study can improve the DCSD PEC presented in Ref. [52].

The information about the ground-state PECs corresponding to the symmetric dissociation of the H_{50} linear chain, as described by the STO-6G basis, which resulted from our CCSD, CCSDT, $\text{ACCSD}(1, \frac{3+4}{2}) = \text{DCSD}$, and $\text{ACCSDT}(1, \frac{3+4}{2})$ calculations, along with the reference LDMRG(500) energetics taken from Ref. [47], is summarized in Table VII and Fig. 4. As one might anticipate, given the large number of strongly correlated electrons, the H_{50} system is much more challenging than the previously discussed H_6 and H_{10} rings. This becomes apparent when we look at the results of the CCSD and CCSDT calculations, which fail to converge already near the equilibrium region, most likely due to the emergence of branch point singularities and the real solutions of the corresponding amplitude equations becoming complex as all H–H bonds of the H_{50} linear chain are simultaneously stretched. As pointed out in Section III A, the singularities and divergences of this kind were observed in the studies of cyclic polyene models reported in Refs. [60–67]. The fact that we could not converge the CCSD and CCSDT amplitudes for the H_{50} system already in the equilibrium region is consistent with the observations made in Refs. [60, 63–65, 67] that the branch point singularities plaguing conventional CC calculations move toward the regions of weaker correlations as the system size increases. The CCSDT method offers significant improvements in the CCSD energies at compressed H–H distances, but this is not helpful, since neither CCSD nor CCSDT solutions can be continued beyond the equilibrium region.

In view of the above failures of the conventional CCSD and CCSDT approaches, it is

encouraging to see that our ACCSDT($1, \frac{3+4}{2}$) scheme provides a non-singular and reliable description of the H_{50} linear chain in the entire range of H–H separations considered in this work, including the H–H bond lengths as large as twice the equilibrium value of R_{H-H} , reducing the MUE relative to the LDMRG(500) reference data that characterizes the already well-behaved ACCSD($1, \frac{3+4}{2}$) = DCSD method, of more than 47 mE_h, to less than 14 mE_h (see Table VII and Fig. 4). The improvements in the results obtained with the lower-rank ACCSD($1, \frac{3+4}{2}$) approach, which neglects T_3 contributions, offered by the ACCSDT($1, \frac{3+4}{2}$) method, which includes them, are especially significant when $R_{H-H} \geq 2.0$ bohr, *i.e.*, when the CCSDT calculations stop converging. While it is possible that the PEC representing the symmetric dissociation of the H_{50} linear chain obtained with ACCSDT($1, \frac{3+4}{2}$) starts behaving erratically when $R_{H-H} \gg 3.6$ bohr, the error reductions compared to ACCSD($1, \frac{3+4}{2}$) in the strongly correlated $R_{H-H} = 2.0$ –3.6 bohr region, from about 34–113 mE_h to 5–22 mE_h, are quite remarkable. The errors relative to the nearly exact LDMRG(500) data obtained in the ACCSDT($1, \frac{3+4}{2}$) calculations for the H_{50} /STO-6G system are larger, in absolute value, than the errors relative to FCI characterizing the ACCSDT($1, \frac{3+4}{2}$) and other ACCSDT computations for the H_6 and H_{10} rings, but we have to keep in mind that H_{50} is much larger than H_6 and H_{10} , so the errors relative to exact or nearly exact computations are expected to be larger too. What is more important is the observation that the ACCSDT($1, \frac{3+4}{2}$) calculations for the dissociating H_{50} /STO-6G linear chain reproduce the LDMRG(500) correlation energies, which we use as a reference in this study, to within 1–2 %. This is a noticeable improvement over the underlying ACCSD($1, \frac{3+4}{2}$) approach, which gives 2–5 % differences with the correlation energies obtained in the LDMRG(500) calculations reported in Ref. [47]. It is encouraging to observe that the ACCSDT($1, \frac{3+4}{2}$) approach and most of the other methods in this category examined in this work, including ACCSDT($1, 3 \times \frac{n_o}{n_o+n_u} + 4 \times \frac{n_u}{n_o+n_u}$) and ACCSDT(1,4) and their active-space variants, are capable of reproducing the exact or nearly exact correlation energies in the strongly correlated systems of the type of the hydrogen clusters discussed here and in Section III A to within 1–2 %, independent of the system size and size of the basis employed in the calculations, substantially improving the corresponding ACCSD computations. The ACCSDT($1, \frac{3+4}{2}$) approach is more expensive than its lower-rank ACCSD($1, \frac{3+4}{2}$) = DCSD counterpart, increasing 0.8 s per iteration on a single core of the Dell machine used in the present study to 482 s, when the H_{50} /STO-6G system is examined. We have to realize, however, that a few minutes per iteration on a single core

for a system containing 50 strongly correlated electrons is an insignificant effort, given the observed improvements in the description of the corresponding PEC over CCSD, CCSDT, and ACCSD($1, \frac{3+4}{2}$) offered by ACCSDT($1, \frac{3+4}{2}$) in the region of stretched H–H distances, not to mention the fact that FCI calculations for H_{50} are not feasible.

IV. CONCLUSIONS

It is well established that the conventional single-reference CCSD, CCSDT, *etc.* hierarchy, in which the cluster operator T is truncated at a given many-body rank, displays an erratic behavior when the number of strongly correlated electrons becomes larger than in typical multi-reference situations in chemistry involving single or double bond breaking. At the same time, traditional multi-reference approaches may become inapplicable due to the prohibitively large dimensionalities of the underlying multi-configurational model spaces when the numbers of active electrons and orbitals become larger. The ACP theories, in which one uses subsets of non-linear $(T_2)^2$ diagrams in the CCD or CCSD amplitude equations, are capable of capturing strong correlations involving the entanglement of larger numbers of electrons, but they neglect the physics associated with the connected triply excited clusters needed for a more quantitative description. Furthermore, the specific combinations of $(T_2)^2$ diagrams that work well in the strongly correlated regime of the minimum-basis-set model systems used in the past to rationalize the ACP methods may not necessarily be optimum when larger basis sets and more substantial dynamical correlations are involved. The objective of this study has been to examine both topics and suggest and test solutions that might help develop better and more quantitative ACP models in the future.

In this work, we dealt with the issue of the missing T_3 physics by combining the selected ACP schemes, including the previously formulated ACCSD(1,3), ACCSD(1,4), and ACCSD($1, \frac{3+4}{2}$) = DCSD approaches and the novel ACCSD($1, 3 \times \frac{n_o}{n_o+n_u} + 4 \times \frac{n_u}{n_o+n_u}$) methodology, in which diagrams (3) and (4) of Fig. 1 are scaled by factors depending on the numbers of occupied (n_o) and unoccupied (n_u) orbitals, with the idea of capturing the leading triply excited cluster amplitudes using active orbitals, which was previously exploited in the CCSDt and similar methods. The resulting ACCSDt(1,3), ACCSDt(1,4), ACCSDt($1, \frac{3+4}{2}$), and ACCSDt($1, 3 \times \frac{n_o}{n_o+n_u} + 4 \times \frac{n_u}{n_o+n_u}$) methods, which are obtained by considering the appropriate subsets of $(T_2)^2$ diagrams in the amplitude equations pro-

jected on the doubly excited determinants within the CCSDt system, their more expensive ACCSDT(1,3), ACCSDT(1,4), ACCSDT(1, $\frac{3+4}{2}$), and ACCSDT(1, $3 \times \frac{n_o}{n_o+n_u} + 4 \times \frac{n_u}{n_o+n_u}$) parents, in which T_3 component is treated fully, obtained from CCSDT, and the underlying ACCSD(1,3), ACCSD(1,4), ACCSD(1, $\frac{3+4}{2}$), and ACCSD(1, $3 \times \frac{n_o}{n_o+n_u} + 4 \times \frac{n_u}{n_o+n_u}$) approximations were implemented and tested using the symmetric dissociations of the H_6 and H_{10} rings, as described by the cc-pVTZ and DZ basis sets, and the H_{50} linear chain treated with STO-6G. We used these three systems as our numerical examples, since the linear chains and rings of the equally spaced hydrogen atoms can be used to model metal-insulator transitions in which the weakly correlated metallic phase at compressed geometries becomes the strong correlated insulator at larger H-H separations. The T_3 -corrected ACCSDt(1, $3 \times \frac{n_o}{n_o+n_u} + 4 \times \frac{n_u}{n_o+n_u}$) and ACCSDT(1, $3 \times \frac{n_o}{n_o+n_u} + 4 \times \frac{n_u}{n_o+n_u}$) schemes and their lower-rank ACCSD(1, $3 \times \frac{n_o}{n_o+n_u} + 4 \times \frac{n_u}{n_o+n_u}$) counterpart, in which the connected triply excited clusters are neglected, were used to investigate if the n_o - and n_u -dependent scaling factors at diagrams (3) and (4) can help to improve accuracies when basis sets are larger than a minimum one. We gauged the performance of the various ACP schemes examined in this work by comparing the resulting PECs for the H_6 /cc-pVTZ, H_{10} /DZ, and H_{50} /STO-6G systems with their exact, FCI (H_6 /cc-pVTZ and H_{10} /DZ) or nearly exact, DMRG (H_{50} /STO-6G) counterparts. The FCI PECs for the symmetric dissociations of the H_6 /cc-pVTZ and H_{10} /DZ ring systems were generated in this work using GAMESS. The reference PEC for the symmetric dissociation of the H_{50} linear chain, as described by the STO-6G basis, was taken from Ref. [47], where the authors used the LDMRG(500) approach. We also included the conventional CCSD, CCSDt, and CCSDT methods in our calculations.

We demonstrated that all ACP approaches examined in this study, without and with the connected triples, provide qualitatively correct PECs, eliminating the erratic and, in the case of H_{10} and H_{50} , singular behavior of CCSD, CCSDt, and CCSDT in the strongly correlated regime. Of all ACP methods including T_3 correlations, the ACCSDt(1, $3 \times \frac{n_o}{n_o+n_u} + 4 \times \frac{n_u}{n_o+n_u}$) approach and its ACCSDT(1, $3 \times \frac{n_o}{n_o+n_u} + 4 \times \frac{n_u}{n_o+n_u}$) parent, which in the minimum-basis-set case become equivalent to ACCSDt(1, $\frac{3+4}{2}$) and ACCSDT(1, $\frac{3+4}{2}$), respectively, turned out to be overall most accurate, improving the corresponding ACCSD(1, $3 \times \frac{n_o}{n_o+n_u} + 4 \times \frac{n_u}{n_o+n_u}$) [in the case of ACCSDt(1, $\frac{3+4}{2}$) and ACCSDT(1, $\frac{3+4}{2}$), ACCSD(1, $\frac{3+4}{2}$) = DCSD] PECs, especially in the regions of larger H-H separations, where correlations become stronger. In general, it was promising to find out that the ACCSDT(1, $3 \times \frac{n_o}{n_o+n_u} + 4 \times \frac{n_u}{n_o+n_u}$), ACCSDT(1,4), and

ACCSDT($1, \frac{3+4}{2}$) methods and their more economical active-space ACCSDt($1, 3 \times \frac{n_o}{n_o+n_u} + 4 \times \frac{n_u}{n_o+n_u}$), ACCSDt(1,4), and ACCSDt($1, \frac{3+4}{2}$) counterparts reproduce the exact or nearly exact correlation energies in the hydrogen clusters, which model transitions from the weakly correlated metallic regime to the strongly correlated insulator phase, to within 1–2 %, reducing errors in the underlying ACCSD computations in a substantial manner. It was also encouraging to observe that all ACCSDt schemes, which use active orbitals that reflect on the nature of strong correlations of interest to identify the dominant T_3 contributions, faithfully reproduce the results of the corresponding ACCSDT calculations, in which the connected three-body clusters are treated fully, at the small fraction of the computational effort. While the n_o - and n_u -dependent scaling factors at diagrams (3) and (4) did not help the ACCSD calculations, they seem to be useful in improving the accuracies of the ACCSDt and ACCSDT computations when larger basis sets are employed. Having said this, there may be other, better ways of improving accuracies of T_3 -corrected ACP approaches in calculations for strongly correlated systems involving the entanglement of larger numbers of electrons and using larger basis sets, and we will search for such ways in the future.

Among the other issues we would like to pursue is search for diagram cancellations within the externally corrected CCSDt and CCSDT amplitude equations projected on triples that would be consistent with the $(T_2)^2$ diagram selections used by the ACP methods in the equations projected on doubles. While some diagram selections within the CCSDT equations were considered in Refs. [147, 148, 151, 159, 160], it remains unclear if the resulting or similar methods can handle strongly correlated systems involving the entanglement of larger numbers of electrons. As pointed out in Section II, model systems that were used in the past to justify the $(T_2)^2$ diagram cancellations defining the ACP schemes by extracting T_4 contributions from the wave functions obtained by projecting out the singlet components of the UHF determinants breaking the S^2 symmetry, but not S_z , do not offer any guidance how to handle T_3 clusters, since the T_n components with odd values of $n \geq 3$ are absent in the resulting PUHF states [125, 126]. In order to see the emergence of T_3 contributions through spin-symmetry breaking and restoration, one has to break the S^2 as well as S_z symmetries, as in Ref. [129]. Thus, it would be worth examining if the considerations reported in Ref. [129] allow one to come up with diagram cancellations or combinations within the CCSDt/CCSDT amplitude equations that could describe strong correlations, as understood throughout the present article, while accounting for the connected triply excited clusters at the same time.

FUNDING

This work has been supported by the Chemical Sciences, Geosciences and Biosciences Division, Office of Basic Energy Sciences, Office of Science, U.S. Department of Energy (Grant No. DE-FG02-01ER15228).

ORCID

Ilias Magoulas <https://orcid.org/0000-0003-3252-9112>

Jun Shen <https://orcid.org/0000-0003-1838-3719>

Piotr Piecuch <https://orcid.org/0000-0002-7207-1815>

-
- [1] J. Hubbard, Proc. R. Soc. London A **240**, 539 (1957).
 - [2] N. M. Hugenholtz, Physica **23**, 481 (1957).
 - [3] F. Coester, Nucl. Phys. **7**, 421 (1958).
 - [4] F. Coester and H. Kümmel, Nucl. Phys. **17**, 477 (1960).
 - [5] J. Čížek, J. Chem. Phys. **45**, 4256 (1966).
 - [6] J. Čížek, Adv. Chem. Phys. **14**, 35 (1969).
 - [7] J. Čížek and J. Paldus, Int. J. Quantum Chem. **5**, 359 (1971).
 - [8] J. Paldus, J. Čížek, and I. Shavitt, Phys. Rev. A **5**, 50 (1972).
 - [9] J. Paldus and X. Li, Adv. Chem. Phys. **110**, 1 (1999).
 - [10] R. J. Bartlett and M. Musiał, Rev. Mod. Phys. **79**, 291 (2007).
 - [11] G. D. Purvis, III and R. J. Bartlett, J. Chem. Phys. **76**, 1910 (1982).
 - [12] J. M. Cullen and M. C. Zerner, J. Chem. Phys. **77**, 4088 (1982).
 - [13] G. E. Scuseria, A. C. Scheiner, T. J. Lee, J. E. Rice, and H. F. Schaefer, III, J. Chem. Phys. **86**, 2881 (1987).
 - [14] P. Piecuch and J. Paldus, Int. J. Quantum Chem. **36**, 429 (1989).
 - [15] J. Noga and R. J. Bartlett, J. Chem. Phys. **86**, 7041 (1987), *ibid.* **89**, 3401 (1988) [Erratum].
 - [16] G. E. Scuseria and H. F. Schaefer, III, Chem. Phys. Lett. **152**, 382 (1988).
 - [17] J. D. Watts and R. J. Bartlett, J. Chem. Phys. **93**, 6104 (1990).

- [18] N. Oliphant and L. Adamowicz, J. Chem. Phys. **95**, 6645 (1991).
- [19] S. A. Kucharski and R. J. Bartlett, Theor. Chim. Acta **80**, 387 (1991).
- [20] S. A. Kucharski and R. J. Bartlett, J. Chem. Phys. **97**, 4282 (1992).
- [21] P. Piecuch and L. Adamowicz, J. Chem. Phys. **100**, 5792 (1994).
- [22] K. Emrich, Nucl. Phys. A **351**, 379 (1981).
- [23] J. Geertsen, M. Rittby, and R. J. Bartlett, Chem. Phys. Lett. **164**, 57 (1989).
- [24] J. F. Stanton and R. J. Bartlett, J. Chem. Phys. **98**, 7029 (1993).
- [25] K. Kowalski and P. Piecuch, J. Chem. Phys. **115**, 643 (2001).
- [26] K. Kowalski and P. Piecuch, Chem. Phys. Lett. **347**, 237 (2001).
- [27] S. A. Kucharski, M. Włoch, M. Musiał, and R. J. Bartlett, J. Chem. Phys. **115**, 8263 (2001).
- [28] M. Kállay and J. Gauss, J. Chem. Phys. **121**, 9257 (2004).
- [29] S. Hirata, J. Chem. Phys. **121**, 51 (2004).
- [30] H. Monkhorst, Int. J. Quantum Chem. Symp. **11**, 421 (1977).
- [31] E. Dalgaard and H. Monkhorst, Phys. Rev. A **28**, 1217 (1983).
- [32] D. Mukherjee and P. K. Mukherjee, Chem. Phys. **39**, 325 (1979).
- [33] H. Sekino and R. J. Bartlett, Int. J. Quantum Chem. Symp. **18**, 255 (1984).
- [34] M. Takahashi and J. Paldus, J. Chem. Phys. **85**, 1486 (1986).
- [35] H. Koch and P. Jørgensen, J. Chem. Phys. **93**, 3333 (1990).
- [36] H. Koch, H. J. A. Jensen, P. Jørgensen, and T. Helgaker, J. Chem. Phys. **93**, 3345 (1990).
- [37] A. E. Kondo, P. Piecuch, and J. Paldus, J. Chem. Phys. **102**, 6511 (1995).
- [38] A. E. Kondo, P. Piecuch, and J. Paldus, J. Chem. Phys. **104**, 8566 (1996).
- [39] N. F. Mott, Proc. Phys. Soc. A **62**, 416 (1949).
- [40] N. F. Mott, Rev. Mod. Phys. **40**, 677 (1968).
- [41] N. F. Mott, *Metal-Insulator Transitions* (Taylor and Francis, London, 1974; 2nd edition 1990, 1990).
- [42] J. Hubbard, Proc. R. Soc. London A **276**, 238 (1963).
- [43] J. Hubbard, Proc. R. Soc. London A **277**, 237 (1964).
- [44] J. Hubbard, Proc. R. Soc. London A **281**, 401 (1964).
- [45] D. Vollhardt, Rev. Mod. Phys. **56**, 99 (1984).
- [46] M. Imada, A. Fujimori, and Y. Tokura, Rev. Mod. Phys. **70**, 1039 (1998).
- [47] J. Hachmann, W. Cardoen, and G. K.-L. Chan, J. Chem. Phys. **125**, 144101 (2006).

- [48] G. L. Bendazzoli, S. Evangelisti, and A. Monari, *Int. J. Quantum Chem.* **111**, 3416 (2011).
- [49] M. Motta, D. M. Ceperley, G. K.-L. Chan, J. A. Gomez, E. Gull, S. Guo, C. A. Jiménez-Hoyos, T. N. Lan, J. Li, F. Ma, A. J. Millis, N. V. Prokof'ev, U. Ray, G. E. Scuseria, S. Sorella, E. M. Stoudenmire, Q. Sun, I. S. Tupitsyn, S. R. White, D. Zgid, and S. Zhang, *Phys. Rev. X* **7**, 031059 (2017).
- [50] T. Tsuchimochi and G. E. Scuseria, *J. Chem. Phys.* **131**, 121102 (2009).
- [51] A. V. Sinititskiy, L. Greenman, and D. A. Mazziotti, *J. Chem. Phys.* **133**, 014104 (2010).
- [52] D. Kats and F. R. Manby, *J. Chem. Phys.* **139**, 021102 (2013).
- [53] E. Pastorczak, J. Shen, M. Hapka, P. Piecuch, and K. Pernal, *J. Chem. Theory Comput.* **13**, 5404 (2017).
- [54] N. H. Stair and F. A. Evangelista, *J. Chem. Phys.* **153**, 104108 (2020).
- [55] R. Pauncz, J. de Heer, and P.-O. Löwdin, *J. Chem. Phys.* **36**, 2247 (1962).
- [56] R. Pauncz, J. de Heer, and P.-O. Löwdin, *J. Chem. Phys.* **36**, 2257 (1962).
- [57] R. Pariser and R. G. Parr, *J. Chem. Phys.* **21**, 466 (1953).
- [58] R. Pariser and R. G. Parr, *J. Chem. Phys.* **21**, 767 (1953).
- [59] J. A. Pople, *Trans. Faraday Soc.* **49**, 1375 (1953).
- [60] J. Paldus, M. Takahashi, and R. W. H. Cho, *Phys. Rev. B* **30**, 4267 (1984).
- [61] J. Paldus, M. Takahashi, and R. W. H. Cho, *Int. J. Quantum Chem. Symp.* **18**, 237 (1984).
- [62] M. Takahashi and J. Paldus, *Phys. Rev. B* **31**, 5121 (1985).
- [63] P. Piecuch, S. Zarrabian, J. Paldus, and J. Čížek, *Phys. Rev. B* **42**, 3351 (1990).
- [64] P. Piecuch and J. Paldus, *Int. J. Quantum Chem. Symp.* **25**, 9 (1991).
- [65] J. Paldus and P. Piecuch, *Int. J. Quantum Chem.* **42**, 135 (1992).
- [66] P. Piecuch, J. Čížek, and J. Paldus, *Int. J. Quantum Chem.* **42**, 165 (1992).
- [67] R. Podeszwa, S. A. Kucharski, and L. Z. Stolarczyk, *J. Chem. Phys.* **116**, 480 (2002).
- [68] I. Lindgren and D. Mukherjee, *Phys. Rep.* **151**, 93 (1987).
- [69] P. Piecuch and K. Kowalski, *Int. J. Mol. Sci.* **3**, 676 (2002).
- [70] D. I. Lyakh, M. Musiał, V. F. Lotrich, and R. J. Bartlett, *Chem. Rev.* **112**, 182 (2012).
- [71] F. A. Evangelista, *J. Chem. Phys.* **149**, 030901 (2018).
- [72] P. G. Szalay, T. Müller, G. Gidofalvi, H. Lischka, and R. Shepard, *Chem. Rev.* **112**, 108 (2012).
- [73] D. Roca-Sanjuán, F. Aquilante, and R. Lindh, *WIREs Comput. Mol. Sci.* **2**, 585 (2012).

- [74] S. Chattopadhyay, R. K. Chaudhuri, U. S. Mahapatra, A. Ghosh, and S. S. Ray, WIREs Comput. Mol. Sci. **6**, 266 (2016).
- [75] K. Ruedenberg, M. W. Schmidt, M. M. Gilbert, and S. T. Elbert, Chem. Phys. **71**, 41 (1982).
- [76] B. O. Roos, Adv. Chem. Phys. **69**, 399 (1987).
- [77] S. R. White, Phys. Rev. Lett. **69**, 2863 (1992).
- [78] S. R. White and R. L. Martin, J. Chem. Phys. **110**, 4127 (1999).
- [79] A. O. Mitrushenkov, G. Fano, F. Ortolani, R. Linguerri, and P. Palmieri, J. Chem. Phys. **115**, 6815 (2001).
- [80] G. K.-L. Chan and M. Head-Gordon, J. Chem. Phys. **116**, 4462 (2002).
- [81] G. K.-L. Chan and S. Sharma, Annu. Rev. Phys. Chem. **62**, 465 (2011).
- [82] S. Keller, M. Dolfi, M. Troyer, and M. Reiher, J. Chem. Phys. **143**, 244118 (2015).
- [83] G. K.-L. Chan, A. Keselman, N. Nakatani, Z. Li, and S. R. White, J. Chem. Phys. **145**, 014102 (2016).
- [84] A. Baiardi and M. Reiher, J. Chem. Phys. **152**, 040903 (2020).
- [85] G. H. Booth, A. J. W. Thom, and A. Alavi, J. Chem. Phys. **131**, 054106 (2009).
- [86] D. Cleland, G. H. Booth, and A. Alavi, J. Chem. Phys. **132**, 041103 (2010).
- [87] W. Dobrautz, S. D. Smart, and A. Alavi, J. Chem. Phys. **151**, 094104 (2019).
- [88] K. Ghanem, A. Y. Lozovoi, and A. Alavi, J. Chem. Phys. **151**, 224108 (2019).
- [89] K. Ghanem, K. Guther, and A. Alavi, J. Chem. Phys. **153**, 224115 (2020).
- [90] J. L. Whitten and M. Hackmeyer, J. Chem. Phys. **51**, 5584 (1969).
- [91] C. F. Bender and E. R. Davidson, Phys. Rev. **183**, 23 (1969).
- [92] B. Huron, J.-P. Malrieu, and P. Rancurel, J. Chem. Phys. **58**, 5745 (1973).
- [93] R. J. Buenker and S. D. Peyerimhoff, Theor. Chim. Acta **35**, 33 (1974).
- [94] J. B. Schriber and F. A. Evangelista, J. Chem. Phys. **144**, 161106 (2016).
- [95] J. B. Schriber and F. A. Evangelista, J. Chem. Theory Comput. **13**, 5354 (2017).
- [96] N. M. Tubman, J. Lee, T. Y. Takeshita, M. Head-Gordon, and K. B. Whaley, J. Chem. Phys. **145**, 044112 (2016).
- [97] N. M. Tubman, C. D. Freeman, D. S. Levine, D. Hait, M. Head-Gordon, and K. B. Whaley, J. Chem. Theory Comput. **16**, 2139 (2020).

- [98] W. Liu and M. R. Hoffmann, J. Chem. Theory Comput. **12**, 1169 (2016), *ibid.* **12**, 3000 (2016) [Erratum].
- [99] N. Zhang, W. Liu, and M. R. Hoffmann, J. Chem. Theory Comput. **16**, 2296 (2020).
- [100] A. A. Holmes, N. M. Tubman, and C. J. Umrigar, J. Chem. Theory Comput. **12**, 3674 (2016).
- [101] S. Sharma, A. A. Holmes, G. Jeanmairet, A. Alavi, and C. J. Umrigar, J. Chem. Theory Comput. **13**, 1595 (2017).
- [102] J. Li, M. Otten, A. A. Holmes, S. Sharma, and C. J. Umrigar, J. Chem. Phys. **149**, 214110 (2018).
- [103] Y. Garniron, A. Scemama, P.-F. Loos, and M. Caffarel, J. Chem. Phys. **147**, 034101 (2017).
- [104] Y. Garniron, T. Applencourt, K. Gasperich, A. Benali, A. Ferte, J. Paquier, B. Pradines, R. Assaraf, P. Reinhardt, J. Toulouse, P. Barbaresco, N. Renon, G. David, J.-P. Malrieu, M. Veril, M. Caffarel, P.-F. Loos, E. Giner, and A. Scemama, J. Chem. Theory Comput. **15**, 3591 (2019).
- [105] P. A. Malmqvist, A. Rendell, and B. O. Roos, J. Phys. Chem. **94**, 5477 (1990).
- [106] J. Ivanic, J. Chem. Phys. **119**, 9364 (2003).
- [107] J. Ivanic, J. Chem. Phys. **119**, 9377 (2003).
- [108] D. Ma, G. Li Manni, and L. Gagliardi, J. Chem. Phys. **135**, 044128 (2011).
- [109] K. D. Vogiatzis, G. Li Manni, S. J. Stoneburner, D. Ma, and L. Gagliardi, J. Chem. Theory Comput. **11**, 3010 (2015).
- [110] M. R. Hermes and L. Gagliardi, J. Chem. Theory Comput. **15**, 972 (2019).
- [111] Y. Kurashige and T. Yanai, J. Chem. Phys. **135**, 094104 (2011).
- [112] S. Guo, M. A. Watson, W. Hu, Q. Sun, and G. K.-L. Chan, J. Chem. Theory Comput. **12**, 1583 (2016).
- [113] N. Nakatani and S. Guo, J. Chem. Phys. **146**, 094102 (2017).
- [114] S. Sharma and G. K.-L. Chan, J. Chem. Phys. **141**, 111101 (2014).
- [115] L. Freitag, S. Knecht, C. Angeli, and M. Reiher, J. Chem. Theory Comput. **13**, 451 (2017).
- [116] D. Ma, G. Li Manni, J. Olsen, and L. Gagliardi, J. Chem. Theory Comput. **12**, 3208 (2016).
- [117] M. Degroote, T. M. Henderson, J. Zhao, J. Dukelsky, and G. E. Scuseria, Phys. Rev. B **93**, 125124 (2016).

- Comput. Theor. Chem. **1116**, 207 (2017).
- [139] A. Marie, F. Kossoski, and P.-F. Loos, J. Chem. Phys. **155**, 104105 (2021).
 - [140] P. Piecuch and J. Paldus, Theor. Chim. Acta **78**, 65 (1990).
 - [141] B. G. Adams, K. Jankowski, and J. Paldus, Phys. Rev. A **24**, 2316 (1981).
 - [142] K. Jankowski and J. Paldus, Int. J. Quantum Chem. **18**, 1243 (1980).
 - [143] B. G. Adams, K. Jankowski, and J. Paldus, Phys. Rev. A **24**, 2330 (1981).
 - [144] R. A. Chiles and C. E. Dykstra, Chem. Phys. Lett. **80**, 69 (1981).
 - [145] S. M. Bachrach, R. A. Chiles, and C. E. Dykstra, J. Chem. Phys. **75**, 2270 (1981).
 - [146] P. Piecuch, R. Toboła, and J. Paldus, Int. J. Quantum Chem. **55**, 133 (1995).
 - [147] R. J. Bartlett and M. Musiał, J. Chem. Phys. **125**, 204105 (2006).
 - [148] M. Musiał and R. J. Bartlett, J. Chem. Phys. **127**, 024106 (2007).
 - [149] M. Nooijen and R. J. Le Roy, J. Molec. Struct.: THEOCHEM **768**, 25 (2006).
 - [150] L. M. J. Huntington and M. Nooijen, J. Chem. Phys. **133**, 184109 (2010).
 - [151] V. Rishi and E. F. Valeev, J. Chem. Phys. **151**, 064102 (2019).
 - [152] D. Kats, J. Chem. Phys. **141**, 061101 (2014).
 - [153] D. Kats, D. Kreplin, H.-J. Werner, and F. R. Manby, J. Chem. Phys. **142**, 064111 (2015).
 - [154] D. Kats, J. Chem. Phys. **144**, 044102 (2016).
 - [155] D. Kats, Mol. Phys. **116**, 1435 (2018).
 - [156] V. Rishi, A. Perera, and R. J. Bartlett, J. Chem. Phys. **144**, 124117 (2016).
 - [157] V. Rishi, A. Perera, M. Nooijen, and R. J. Bartlett, J. Chem. Phys. **146**, 144104 (2017).
 - [158] V. Rishi, A. Perera, and R. J. Bartlett, Mol. Phys. **117**, 2201 (2019).
 - [159] D. Kats and A. Köhn, J. Chem. Phys. **150**, 151101 (2019).
 - [160] T. Schraivogel and D. Kats, J. Chem. Phys. **155**, 064101 (2021).
 - [161] J. Paldus, J. Math. Chem. **55**, 477 (2017).
 - [162] P. Piecuch, A. E. Kondo, V. Špirko, and J. Paldus, J. Chem. Phys. **104**, 4699 (1996).
 - [163] P. Piecuch, R. Toboła, and J. Paldus, Chem. Phys. Lett. **210**, 243 (1993).
 - [164] K. Raghavachari, J. Chem. Phys. **82**, 4607 (1985).
 - [165] M. Urban, J. Noga, S. J. Cole, and R. J. Bartlett, J. Chem. Phys. **83**, 4041 (1985), *ibid.* **85**, 5383 (1986) [Erratum].
 - [166] K. Raghavachari, G. W. Trucks, J. A. Pople, and M. Head-Gordon, Chem. Phys. Lett. **157**, 479 (1989).

- [167] Y. S. Lee and R. J. Bartlett, J. Chem. Phys. **80**, 4371 (1984).
- [168] Y. S. Lee, S. A. Kucharski, and R. J. Bartlett, J. Chem. Phys. **81**, 5906 (1984), *ibid.* **82**, 5761 (1985) [Erratum].
- [169] N. Oliphant and L. Adamowicz, J. Chem. Phys. **94**, 1229 (1991).
- [170] N. Oliphant and L. Adamowicz, J. Chem. Phys. **96**, 3739 (1992).
- [171] P. Piecuch, N. Oliphant, and L. Adamowicz, J. Chem. Phys. **99**, 1875 (1993).
- [172] P. Piecuch and L. Adamowicz, Chem. Phys. Lett. **221**, 121 (1994).
- [173] P. Piecuch and L. Adamowicz, J. Chem. Phys. **102**, 898 (1995).
- [174] V. Alexandrov, P. Piecuch, and L. Adamowicz, J. Chem. Phys. **102**, 3301 (1995).
- [175] K. B. Ghose, P. Piecuch, and L. Adamowicz, J. Chem. Phys. **103**, 9331 (1995).
- [176] K. B. Ghose, P. Piecuch, S. Pal, and L. Adamowicz, J. Chem. Phys. **104**, 6582 (1996).
- [177] P. Piecuch, S. A. Kucharski, and R. J. Bartlett, J. Chem. Phys. **110**, 6103 (1999).
- [178] P. Piecuch, S. A. Kucharski, and V. Špirko, J. Chem. Phys. **111**, 6679 (1999).
- [179] K. Kowalski and P. Piecuch, Chem. Phys. Lett. **344**, 165 (2001).
- [180] K. Kowalski and P. Piecuch, J. Chem. Phys. **113**, 8490 (2000).
- [181] K. Kowalski, S. Hirata, M. Włoch, P. Piecuch, and T. L. Windus, J. Chem. Phys. **123**, 074319 (2005).
- [182] P. Piecuch, S. Hirata, K. Kowalski, P.-D. Fan, and T. L. Windus, Int. J. Quantum Chem. **106**, 79 (2006).
- [183] J. R. Gour, P. Piecuch, and M. Włoch, J. Chem. Phys. **123**, 134113 (2005).
- [184] J. R. Gour, P. Piecuch, and M. Włoch, Int. J. Quantum Chem. **106**, 2854 (2006).
- [185] J. R. Gour and P. Piecuch, J. Chem. Phys. **125**, 234107 (2006).
- [186] P. Piecuch, Mol. Phys. **108**, 2987 (2010).
- [187] J. Shen and P. Piecuch, J. Chem. Phys. **138**, 194102 (2013).
- [188] J. Shen and P. Piecuch, Mol. Phys. **112**, 868 (2014).
- [189] A. O. Ajala, J. Shen, and P. Piecuch, J. Phys. Chem. A **121**, 3469 (2017).
- [190] J. Čížek, Theor. Chim. Acta **6**, 292 (1966).
- [191] J. Paldus, B. G. Adams, and J. Čížek, Int. J. Quantum Chem. **11**, 813 (1977).
- [192] J. Paldus, J. Chem. Phys. **67**, 303 (1977).
- [193] B. G. Adams and J. Paldus, Phys. Rev. A **20**, 1 (1979).
- [194] R. A. Chiles and C. E. Dykstra, J. Chem. Phys. **74**, 4544 (1981).

- [195] J. Geertsen, S. Eriksen, and J. Oddershede, *Adv. Quantum Chem.* **22**, 167 (1991).
- [196] P. Piecuch and J. Paldus, *Theor. Chim. Acta* **83**, 69 (1992).
- [197] P. Piecuch and J. Paldus, *J. Chem. Phys.* **101**, 5875 (1994).
- [198] J. Paldus and J. Planelles, *Theor. Chim. Acta* **89**, 13 (1994).
- [199] L. Z. Stolarczyk, *Chem. Phys. Lett.* **217**, 1 (1994).
- [200] G. Peris, J. Planelles, and J. Paldus, *Int. J. Quantum Chem.* **62**, 137 (1997).
- [201] G. Peris, J. Planelles, J.-P. Malrieu, and J. Paldus, *J. Chem. Phys.* **110**, 11708 (1999).
- [202] X. Li and J. Paldus, *J. Chem. Phys.* **107**, 6257 (1997).
- [203] X. Li and J. Paldus, *J. Chem. Phys.* **108**, 637 (1998).
- [204] X. Li and J. Paldus, *J. Chem. Phys.* **124**, 174101 (2006).
- [205] E. Xu and S. Li, *J. Chem. Phys.* **142**, 094119 (2015).
- [206] J. E. Deustua, I. Magoulas, J. Shen, and P. Piecuch, *J. Chem. Phys.* **149**, 151101 (2018).
- [207] G. J. R. Aroeira, M. M. Davis, J. M. Turney, and H. F. Schaefer, III, *J. Chem. Theory Comput.* **17**, 182 (2021).
- [208] S. Lee, H. Zhai, S. Sharma, C. J. Umrigar, and G. K.-L. Chan, *J. Chem. Theory Comput.* **17**, 3414 (2021).
- [209] I. Magoulas, K. Gururangan, P. Piecuch, J. E. Deustua, and J. Shen, *J. Chem. Theory Comput.* **17**, 4006 (2021).
- [210] M. W. Schmidt, K. K. Baldridge, J. A. Boatz, S. T. Elbert, M. S. Gordon, J. H. Jensen, S. Koseki, N. Matsunaga, K. A. Nguyen, S. Su, T. L. Windus, M. Dupuis, and J. A. Montgomery, Jr., *J. Comput. Chem.* **14**, 1347 (1993).
- [211] M. S. Gordon and M. W. Schmidt, in *Theory and Applications of Computational Chemistry: The First Forty Years*, edited by C. E. Dykstra, G. Frenking, K. S. Kim, and G. E. Scuseria (Elsevier, Amsterdam, 2005) pp. 1167–1189.
- [212] G. M. J. Barca, C. Bertoni, L. Carrington, D. Datta, N. De Silva, J. E. Deustua, D. G. Fedorov, J. R. Gour, A. O. Gunina, E. Guidez, T. Harville, S. Irle, J. Ivanic, K. Kowalski, S. S. Leang, H. Li, W. Li, J. J. Lutz, I. Magoulas, J. Mato, V. Mironov, H. Nakata, B. Q. Pham, P. Piecuch, D. Poole, S. R. Pruitt, A. P. Rendell, L. B. Roskop, K. Ruedenberg, T. Sattasathuchana, M. W. Schmidt, J. Shen, L. Slipchenko, M. Sosonkina, V. Sundriyal, A. Tiwari, J. L. Galvez Vallejo, B. Westheimer, M. Włoch, P. Xu, F. Zahariev, and M. S. Gordon, *J. Chem. Phys.* **152**, 154102 (2020).

- [213] J. Shen and P. Piecuch, Chem. Phys. **401**, 180 (2012).
- [214] J. Shen and P. Piecuch, J. Chem. Phys. **136**, 144104 (2012).
- [215] J. Shen and P. Piecuch, J. Chem. Theory Comput. **8**, 4968 (2012).
- [216] N. P. Bauman, J. Shen, and P. Piecuch, Mol. Phys. **115**, 2860 (2017).
- [217] J. Ivanic and K. Ruedenberg, Theor. Chem. Acc. **106**, 339 (2001).
- [218] T. H. Dunning, Jr., J. Chem. Phys. **90**, 1007 (1989).
- [219] T. H. Dunning, Jr., J. Chem. Phys. **53**, 2823 (1970).
- [220] T. H. Dunning, Jr. and P. J. Hay, in *Methods of Electronic Structure Theory*, edited by H. F. Schaefer, III (Springer, Boston, 1977) pp. 1–27.
- [221] W. J. Hehre, R. F. Stewart, and J. A. Pople, J. Chem. Phys. **51**, 2657 (1969).

TABLE I. A comparison of the energies obtained with the CCSD and various ACCSD approaches with the exact FCI data for the symmetric dissociation of the H_6 ring, as described by the cc-pVTZ basis set, at selected bond distances between neighboring H atoms R_{H-H} (in Å).^a

R_{H-H}	CCSD	ACCSD				FCI
		(1,3)	$(1, \frac{3+4}{2})^b$	$(1, 3 \times \frac{n_o}{n_o+n_u} + 4 \times \frac{n_u}{n_o+n_u})$	(1,4)	
0.6	3.422	-0.242	1.557	3.144	3.262	-2.858958
0.7	3.593	-0.320	1.618	3.321	3.448	-3.176147
0.8	3.823	-0.417	1.695	3.541	3.679	-3.331124
0.9	4.103	-0.534	1.788	3.809	3.959	-3.396176
1.0	4.424	-0.665	1.906	4.132	4.297	-3.410069
1.1	4.774	-0.805	2.059	4.522	4.705	-3.394673
1.2	5.139	-0.944	2.263	5.003	5.206	-3.362943
1.3	5.489	-1.068	2.543	5.608	5.833	-3.322850
1.4	5.758	-1.156	2.934	6.381	6.634	-3.279466
1.5	5.802	-1.175	3.479	7.377	7.662	-3.236119
1.6	5.309	-1.088	4.219	8.638	8.960	-3.195040
1.7	3.647	-0.865	5.165	10.165	10.529	-3.157716
1.8	-0.380	-0.508	6.266	11.872	12.280	-3.125051
1.9	-8.826	-0.071	7.388	13.563	14.012	-3.097433
2.0	-24.720	0.350	8.337	14.963	15.445	-3.074787
2.1	-51.331	0.660	8.931	15.813	16.314	-3.056686
2.2	-89.837	0.803	9.073	15.975	16.478	-3.042507
2.3	-137.197	0.782	8.776	15.463	15.951	-3.031571
2.4	-187.824	0.635	8.135	14.417	14.876	-3.023237
2.5	-237.074	0.416	7.277	13.027	13.447	-3.016948
MUE ^c	39.624	0.675	4.770	9.037	9.349	—
MSE ^d	-34.095	-0.311	4.770	9.037	9.349	—

^a The FCI energies are total energies in hartree, whereas all of the remaining energies are errors relative to FCI in millihartree.

^b Equivalent to the DCSD approach of Ref. [52].

^c Mean unsigned error.

^d Mean signed error.

TABLE II. A comparison of the energies obtained with the CCSDt and various ACCSDt approaches with the exact FCI data for the symmetric dissociation of the H₆ ring, as described by the cc-pVTZ basis set, at selected bond distances between neighboring H atoms $R_{\text{H-H}}$ (in Å).^a

$R_{\text{H-H}}$	CCSDt	ACCSDt				FCI
		(1,3)	$(1, \frac{3+4}{2})$	$(1, 3 \times \frac{n_o}{n_o+n_u} + 4 \times \frac{n_u}{n_o+n_u})$	(1,4)	
0.6	2.548	-1.234	0.615	2.243	2.365	-2.858958
0.7	2.419	-1.660	0.345	2.103	2.235	-3.176147
0.8	2.235	-2.247	-0.043	1.880	2.023	-3.331124
0.9	2.018	-2.962	-0.515	1.608	1.766	-3.396176
1.0	1.804	-3.757	-1.021	1.339	1.514	-3.410069
1.1	1.609	-4.592	-1.519	1.114	1.309	-3.394673
1.2	1.414	-5.454	-1.992	0.953	1.170	-3.362943
1.3	1.111	-6.428	-2.504	0.809	1.053	-3.322850
1.4	0.669	-7.437	-2.974	0.766	1.040	-3.279466
1.5	-0.074	-8.459	-3.375	0.855	1.163	-3.236119
1.6	-1.438	-9.451	-3.673	1.104	1.451	-3.195040
1.7	-4.014	-10.345	-3.837	1.516	1.904	-3.157716
1.8	-8.888	-11.062	-3.852	2.051	2.478	-3.125051
1.9	-17.983	-11.538	-3.744	2.611	3.069	-3.097433
2.0	-34.481	-11.755	-3.576	3.059	3.535	-3.074787
2.1	-62.336	-11.747	-3.432	3.266	3.744	-3.056686
2.2	-102.675	-11.583	-3.387	3.160	3.624	-3.042507
2.3	-150.692	-11.337	-3.483	2.735	3.172	-3.031571
2.4	-199.899	-11.068	-3.726	2.041	2.442	-3.023237
2.5	-246.321	-10.805	-4.094	1.154	1.516	-3.016948
MUE ^b	42.231	7.746	2.585	1.818	2.129	—
MSE ^c	-40.649	-7.746	-2.489	1.818	2.129	—

^a The FCI energies are total energies in hartree, whereas all of the remaining energies are errors relative to FCI in millihartree. The CCSDt and ACCSDt approaches employed three active occupied and three active unoccupied MOs corresponding to the 1s shells of the individual H atoms.

^b Mean unsigned error.

^c Mean signed error.

TABLE III. A comparison of the energies obtained with the CCSDT and various ACCSDT approaches with the exact FCI data for the symmetric dissociation of the H_6 ring, as described by the cc-pVTZ basis set, at selected bond distances between neighboring H atoms R_{H-H} (in Å).^a

R_{H-H}	CCSDT	ACCSDT				FCI
		(1,3)	$(1, \frac{3+4}{2})$	$(1, 3 \times \frac{n_o}{n_o+n_u} + 4 \times \frac{n_u}{n_o+n_u})$	(1,4)	
0.6	0.079	-3.952	-1.996	-0.279	-0.151	-2.858958
0.7	0.095	-4.233	-2.123	-0.277	-0.139	-3.176147
0.8	0.116	-4.609	-2.304	-0.295	-0.146	-3.331124
0.9	0.140	-5.074	-2.530	-0.325	-0.162	-3.396176
1.0	0.160	-5.621	-2.792	-0.356	-0.175	-3.410069
1.1	0.166	-6.241	-3.079	-0.374	-0.174	-3.394673
1.2	0.137	-6.932	-3.381	-0.365	-0.143	-3.362943
1.3	0.031	-7.692	-3.686	-0.307	-0.059	-3.322850
1.4	-0.235	-8.512	-3.973	-0.172	0.106	-3.279466
1.5	-0.823	-9.369	-4.213	0.072	0.385	-3.236119
1.6	-2.046	-10.216	-4.371	0.457	0.808	-3.195040
1.7	-4.493	-10.982	-4.411	0.989	1.380	-3.157716
1.8	-9.245	-11.585	-4.316	1.631	2.061	-3.125051
1.9	-18.225	-11.959	-4.109	2.286	2.747	-3.097433
2.0	-34.617	-12.084	-3.855	2.817	3.296	-3.074787
2.1	-62.392	-11.995	-3.635	3.095	3.576	-3.056686
2.2	-102.685	-11.760	-3.526	3.048	3.514	-3.042507
2.3	-150.676	-11.452	-3.567	2.673	3.111	-3.031571
2.4	-199.857	-11.129	-3.764	2.019	2.421	-3.023237
2.5	-246.248	-10.820	-4.092	1.165	1.528	-3.016948
MUE ^b	41.623	8.811	3.486	1.150	1.304	—
MSE ^c	-41.531	-8.811	-3.486	0.875	1.189	—

^a The FCI energies are total energies in hartree, whereas all of the remaining energies are errors relative to FCI in millihartree.

^b Mean unsigned error.

^c Mean signed error.

TABLE IV. A comparison of the energies obtained with the CCSD and various ACCSD approaches with the exact FCI data for the symmetric dissociation of the H₁₀ ring, as described by the DZ basis set, at selected bond distances between neighboring H atoms $R_{\text{H-H}}$ (in Å).^a

$R_{\text{H-H}}$	CCSD	ACCSD				FCI
		(1,3)	$(1, \frac{3+4}{2})^b$	$(1, 3 \times \frac{n_o}{n_o+n_u} + 4 \times \frac{n_u}{n_o+n_u})$	(1,4)	
0.6	2.461	0.412	0.945	1.204	1.458	-4.581177
0.7	2.942	0.498	1.071	1.348	1.619	-5.133564
0.8	3.519	0.708	1.314	1.606	1.890	-5.400721
0.9	4.157	1.053	1.689	1.992	2.285	-5.513021
1.0	4.878	1.591	2.265	2.582	2.886	-5.538852
1.1	5.691	2.435	3.164	3.501	3.821	-5.516586
1.2	6.510	3.744	4.552	4.917	5.257	-5.468944
1.3	7.013	5.701	6.620	7.022	7.388	-5.409818
1.4	6.288	8.451	9.520	9.972	10.370	-5.347723
1.5	1.896	11.987	13.258	13.773	14.209	-5.287756
1.6	-13.106	16.041	17.575	18.168	18.647	-5.232798
1.7	-66.276	20.069	21.930	22.618	23.144	-5.184271
1.8	NC ^c	23.410	25.650	26.446	27.026	-5.142644
1.9	NC ^c	25.531	28.163	29.075	29.715	-5.107796
2.0	NC ^c	26.191	29.172	30.197	30.903	-5.079254
2.1	NC ^c	25.462	28.691	29.809	30.585	-5.056349
2.2	NC ^c	23.636	26.967	28.146	28.985	-5.038308
2.3	NC ^c	21.090	24.372	25.568	26.453	-5.024332
2.4	NC ^c	18.193	21.298	22.468	23.370	-5.013655
2.5	NC ^c	15.248	18.087	19.193	20.080	-5.005591
MUE ^d	NA ^e	12.572	14.315	14.980	15.505	—
MSE ^f	NA ^e	12.572	14.315	14.980	15.505	—

^a The FCI energies are total energies in hartree, whereas all of the remaining energies are errors relative to FCI in millihartree.

^b Equivalent to the DCSD approach of Ref. [52].

^c No convergence.

^d Mean unsigned error.

^e The mean errors are not reported because CCSD does not converge at larger values of $R_{\text{H-H}}$.

^f Mean signed error.

TABLE V. A comparison of the energies obtained with the CCSDt and various ACCSDt approaches with the exact FCI data for the symmetric dissociation of the H₁₀ ring, as described by the DZ basis set, at selected bond distances between neighboring H atoms $R_{\text{H-H}}$ (in Å).^a

$R_{\text{H-H}}$	CCSDt	ACCSDt				FCI
		(1,3)	(1, $\frac{3+4}{2}$)	(1, $3 \times \frac{n_o}{n_o+n_u} + 4 \times \frac{n_u}{n_o+n_u}$)	(1,4)	
0.6	0.455	-1.751	-1.181	-0.904	-0.633	-4.581177
0.7	0.554	-2.110	-1.502	-1.209	-0.922	-5.133564
0.8	0.416	-2.726	-2.081	-1.773	-1.473	-5.400721
0.9	0.349	-3.218	-2.541	-2.221	-1.912	-5.513021
1.0	0.181	-3.735	-3.019	-2.686	-2.369	-5.538852
1.1	-0.084	-4.169	-3.399	-3.050	-2.724	-5.516586
1.2	-0.650	-4.477	-3.634	-3.266	-2.933	-5.468944
1.3	-1.956	-4.591	-3.654	-3.266	-2.931	-5.409818
1.4	-4.961	-4.457	-3.399	-2.994	-2.672	-5.347723
1.5	-11.879	-4.091	-2.881	-2.468	-2.182	-5.287756
1.6	-28.679	-3.630	-2.233	-1.824	-1.609	-5.232798
1.7	-81.643	-3.315	-1.692	-1.300	-1.193	-5.184271
1.8	NC ^b	-3.398	-1.510	-1.144	-1.178	-5.142644
1.9	NC ^b	-4.043	-1.862	-1.523	-1.712	-5.107796
2.0	NC ^b	-5.295	-2.810	-2.494	-2.832	-5.079254
2.1	NC ^b	-7.106	-4.333	-4.029	-4.497	-5.056349
2.2	NC ^b	-9.380	-6.355	-6.055	-6.626	-5.038308
2.3	NC ^b	-12.001	-8.762	-8.462	-9.114	-5.024332
2.4	NC ^b	-14.806	-11.381	-11.083	-11.806	-5.013655
2.5	NC ^b	-17.551	-13.966	-13.660	-14.471	-5.005591
MUE ^c	NA ^d	5.793	4.110	3.770	3.790	—
MSE ^e	NA ^d	-5.793	-4.110	-3.770	-3.790	—

^a The FCI energies are total energies in hartree, whereas all of the remaining energies are errors relative to FCI in millihartree. The CCSDt and ACCSDt approaches employed five active occupied and five active unoccupied MOs corresponding to the 1s shells of the individual H atoms.

^b No convergence.

^c Mean unsigned error.

^d The mean errors are not reported because CCSDt does not converge at larger values of $R_{\text{H-H}}$.

^e Mean signed error.

TABLE VI. A comparison of the energies obtained with the CCSDT and various ACCSDT approaches with the exact FCI data for the symmetric dissociation of the H₁₀ ring, as described by the DZ basis set, at selected bond distances between neighboring H atoms $R_{\text{H-H}}$ (in Å).^a

$R_{\text{H-H}}$	CCSDT	ACCSDT				FCI
		(1,3)	$(1, \frac{3+4}{2})$	$(1, 3 \times \frac{n_o}{n_o+n_u} + 4 \times \frac{n_u}{n_o+n_u})$	(1,4)	
0.6	0.065	-2.167	-1.591	-1.311	-1.037	-4.581177
0.7	0.094	-2.602	-1.986	-1.688	-1.398	-5.133564
0.8	0.110	-3.054	-2.404	-2.093	-1.790	-5.400721
0.9	0.101	-3.485	-2.805	-2.482	-2.172	-5.513021
1.0	0.035	-3.894	-3.175	-2.841	-2.523	-5.538852
1.1	-0.170	-4.262	-3.491	-3.141	-2.815	-5.516586
1.2	-0.703	-4.535	-3.691	-3.323	-2.989	-5.468944
1.3	-1.991	-4.631	-3.693	-3.305	-2.969	-5.409818
1.4	-4.986	-4.487	-3.428	-3.023	-2.700	-5.347723
1.5	-11.897	-4.115	-2.904	-2.490	-2.205	-5.287756
1.6	-28.687	-3.649	-2.251	-1.842	-1.626	-5.232798
1.7	-81.631	-3.330	-1.706	-1.313	-1.206	-5.184271
1.8	NC ^b	-3.408	-1.520	-1.153	-1.187	-5.142644
1.9	NC ^b	-4.049	-1.867	-1.528	-1.717	-5.107796
2.0	NC ^b	-5.296	-2.811	-2.494	-2.833	-5.079254
2.1	NC ^b	-7.101	-4.329	-4.025	-4.493	-5.056349
2.2	NC ^b	-9.371	-6.346	-6.045	-6.618	-5.038308
2.3	NC ^b	-11.988	-8.750	-8.449	-9.100	-5.024332
2.4	NC ^b	-14.790	-11.365	-11.068	-11.791	-5.013655
2.5	NC ^b	-17.533	-13.927	-13.644	-14.459	-5.005591
MUE ^c	NA ^d	5.887	4.202	3.863	3.881	—
MSE ^e	NA ^d	-5.887	-4.202	-3.863	-3.881	—

^a The FCI energies are total energies in hartree, whereas all of the remaining energies are errors relative to FCI in millihartree.

^b No convergence.

^c Mean unsigned error.

^d The mean errors are not reported because CCSDT does not converge at larger values of $R_{\text{H-H}}$.

^e Mean signed error.

TABLE VII. A comparison of the energies obtained with the CCSD, ACCSD($1, \frac{3+4}{2}$) = DCSD, CCSDT, and ACCSDT($1, \frac{3+4}{2}$) approaches with the nearly exact LDMRG(500) data for the symmetric dissociation of the H_{50} linear chain, as described by the STO-6G basis set, at selected bond distances between neighboring H atoms R_{H-H} (in bohr).^a

R_{H-H}	CCSD	ACCSD($1, \frac{3+4}{2}$)	CCSDT	ACCSDT($1, \frac{3+4}{2}$)	LDMRG(500)
1.0	11.90	6.30	0.27	-6.68	-17.28407
1.2	16.28	9.12	0.29	-9.08	-22.94765
1.4	20.99	12.78	-0.10	-11.37	-25.59378
1.6	26.01	17.82	-1.71	-13.26	-26.71944
1.8	31.00	24.87	-6.96	-14.62	-27.03865
2.0	34.60	34.30	NC ^b	-15.73	-26.92609
2.4	NC ^b	59.23	NC ^b	-22.04 ^c	-26.16057
2.8	NC ^b	86.24	NC ^b	-22.47 ^d	-25.27480
3.2	NC ^b	106.45	NC ^b	-18.78 ^d	-24.56828
3.6	NC ^b	113.43	NC ^b	-4.66 ^d	-24.10277
MUE ^e	NA ^f	47.05	NA ^g	13.87	—
MSE ^h	NA ^f	47.05	NA ^g	-13.87	—

^a The LDMRG(500) energies, taken from Ref. [47], are total energies in hartree. The remaining energies are errors relative to LDMRG(500) in millihartree. In this case $n_o = n_u$, so that

$$\text{ACCSD}(1, 3 \times \frac{n_o}{n_o + n_u} + 4 \times \frac{n_u}{n_o + n_u}) = \text{ACCSD}(1, \frac{3+4}{2}) = \text{DCSD} \text{ and}$$

$$\text{ACCSDT}(1, 3 \times \frac{n_o}{n_o + n_u} + 4 \times \frac{n_u}{n_o + n_u}) = \text{ACCSDT}(1, \frac{3+4}{2}).$$

^b No convergence.

^c We were unable to converge this energy to an accuracy better than 1 mE_h. The reported value corresponds to the last CC iteration.

^d We were unable to converge this energy to an accuracy better than 0.1 mE_h. The reported value corresponds to the last CC iteration.

^e Mean unsigned error.

^f The mean errors are not reported because CCSD does not converge at larger values of R_{H-H} .

^g The mean errors are not reported because CCSDT does not converge at larger values of R_{H-H} .

^h Mean signed error.

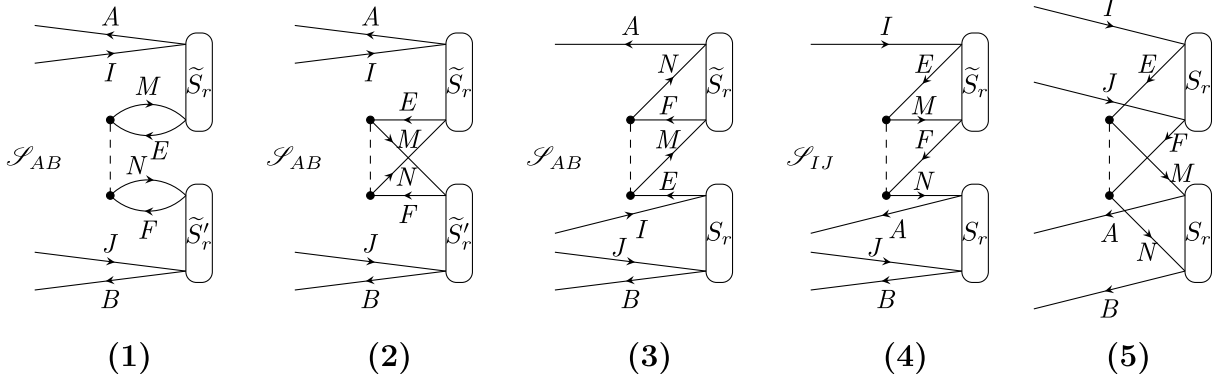


FIG. 1. Goldstone–Brandow orbital diagrams for the $(T_2)^2$ contributions $\Lambda_k^{(2)}(AB, IJ; S_r)$, $k = 1-5$, to the CCD or CCSD equations projected on the singlet pp–hh coupled orthogonally spin-adapted doubly excited $|\Phi_{IJ}^{AB}\rangle_{S_r}$ states. The intermediate spin quantum number S_r in the definition of the $|\Phi_{IJ}^{AB}\rangle_{S_r}$ states and the associated doubly excited cluster amplitudes $t_{AB}^{IJ}(S_r)$ in the definition of the orthogonally spin-adapted T_2 operators, represented by the Brandow-type, oval-shaped vertices, is 0 or 1. The occupied orbital indices M and N , the unoccupied orbital indices E and F , and the intermediate spin quantum numbers \tilde{S}_r and \tilde{S}'_r are summed over. The $\mathcal{S}_{AB} = 1 + (AB)$ and $\mathcal{S}_{IJ} = 1 + (IJ)$ operators at the diagrams are index symmetrizers that translate into the symmetrizers or antisymmetrizers, $\mathcal{S}_{AB}(S_r) = 1 + (-1)^{S_r}(AB)$ and $\mathcal{S}_{IJ}(S_r) = 1 + (-1)^{S_r}(IJ)$, respectively, in the resulting algebraic expressions.

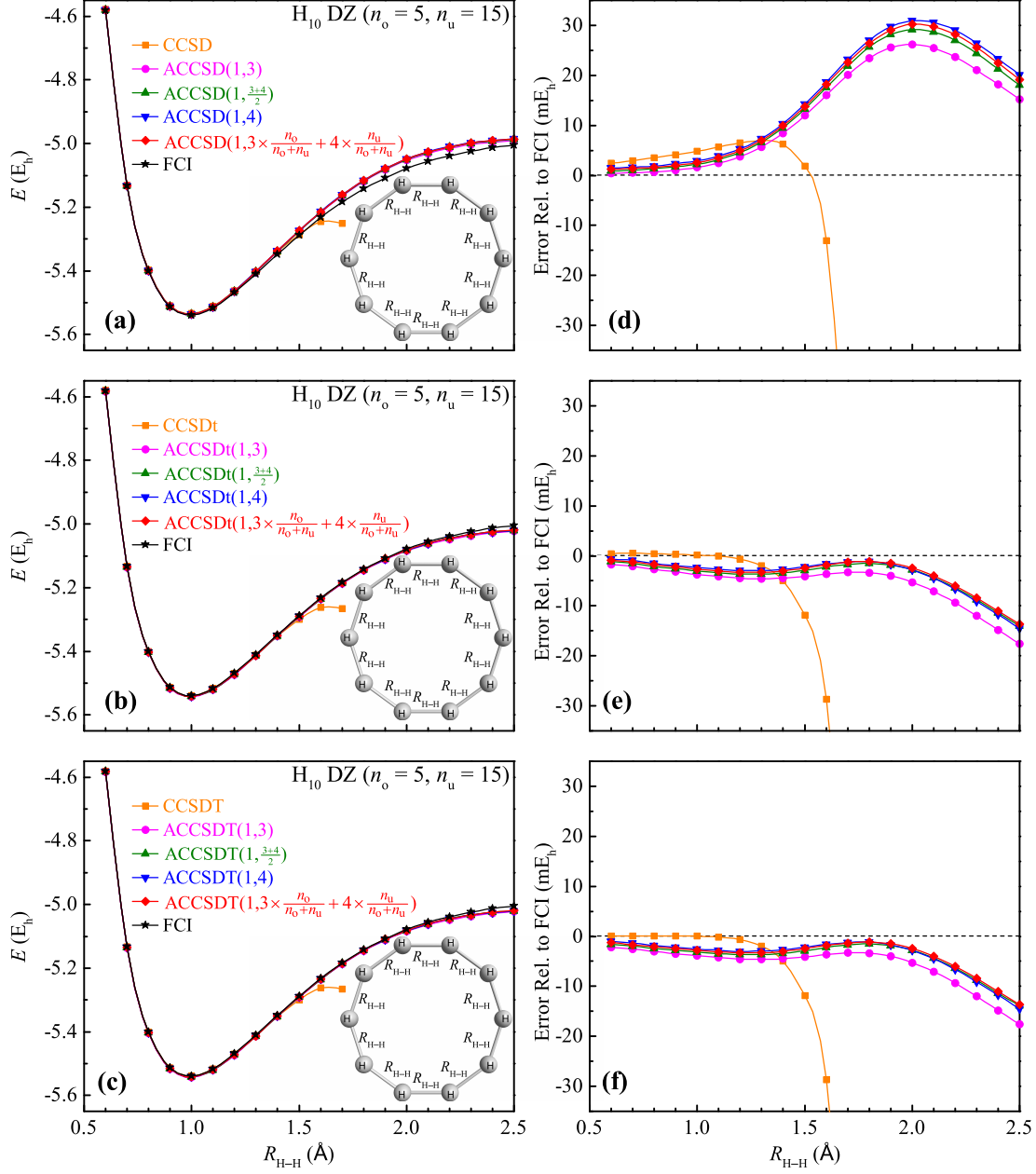


FIG. 3. Ground-state PECs [panels (a)–(c)] and errors relative to FCI [panels (d)–(f)] for the symmetric dissociation of the H_{10} ring resulting from the CCSD and various ACCSD [panels (a) and (d)], CCSDt and various ACCSDt [panels (b) and (e)], and CCSDT and various ACCSDT [panels (c) and (f)] calculations using the DZ basis set. The CCSDt and ACCSDt approaches employed a minimum active space consisting of five occupied and five lowest-energy unoccupied MOs that correlate with the $1s$ shells of the individual hydrogen atoms. The FCI PEC included in panels (a)–(c) is shown to facilitate comparisons. Note that the CCSD, CCSDt, and CCSDT calculations failed to converge in the $R_{H-H} \geq 1.8$ Å region.

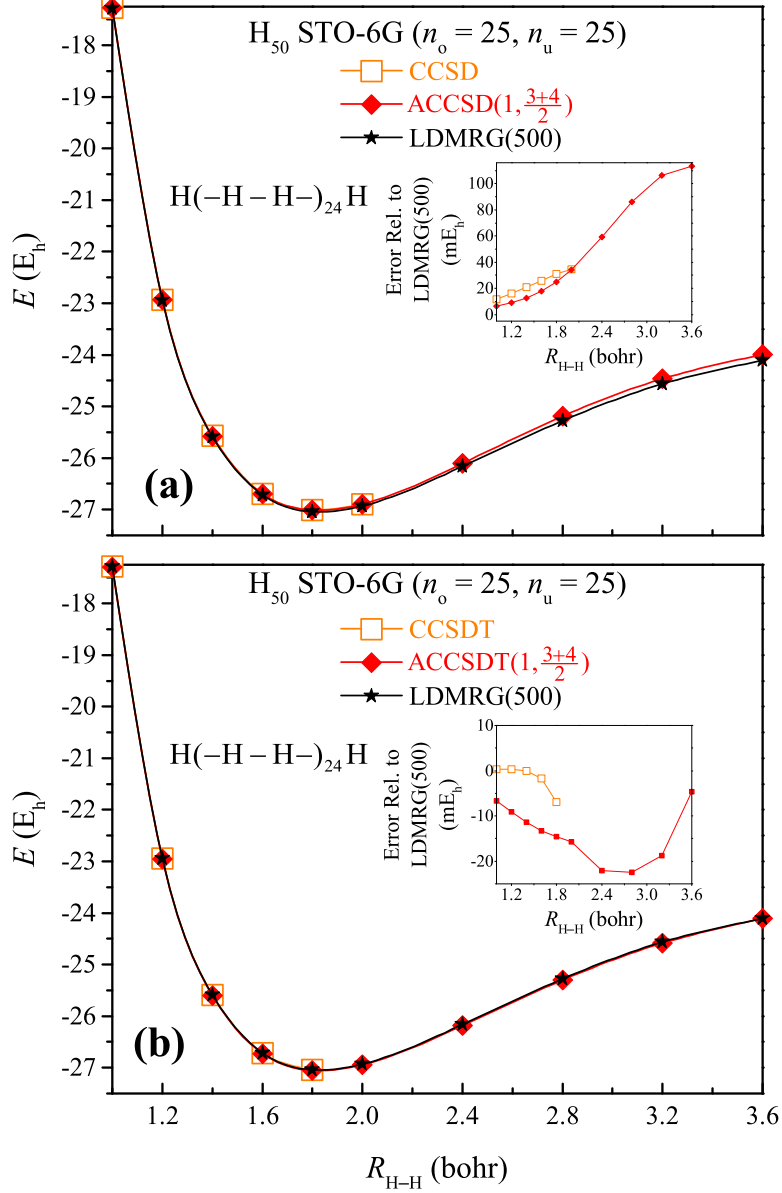


FIG. 4. Ground-state PECs for the symmetric dissociation of the H_{50} linear chain obtained in the (a) CCSD and ACCSD($1, \frac{3+4}{2}$) and (b) CCSDT and ACCSDT($1, \frac{3+4}{2}$) calculations using the STO-6G basis set. In this case $n_o = n_u = N_o = N_u$, so that ACCSD($1, \frac{3+4}{2}$) = DCSD is equivalent to ACCSD($1, 3 \times \frac{n_o}{n_o+n_u} + 4 \times \frac{n_u}{n_o+n_u}$) and ACCSDT($1, \frac{3+4}{2}$) is equivalent to ACCSDt($1, \frac{3+4}{2}$), ACCSDt($1, 3 \times \frac{n_o}{n_o+n_u} + 4 \times \frac{n_u}{n_o+n_u}$), and ACCSDT($1, 3 \times \frac{n_o}{n_o+n_u} + 4 \times \frac{n_u}{n_o+n_u}$). The LDMRG(500) PEC included for comparison purposes is based on the data reported in Ref. [47]. The insets show the errors relative to LDMRG(500). Note that the CCSD calculations failed to converge in the $R_{H-H} > 2.0$ bohr region. We could not converge the CCSDT equations beyond $R_{H-H} = 1.8$ bohr.